AN INVESTIGATION OF GRADING MARGIN VIOLATION IN COORDINATING OVERCURRENT RELAY

CHAN KOK WAI

FACULTY OF ENGINEERING
UNIVERSITY OF MALAYA
KUALA LUMPUR

2019

AN INVESTIGATION OF GRADING MARGIN VIOLATION IN COORDINATING OVERCURRENT RELAY

CHAN KOK WAI

RESEARCH REPORT SUBMITTED TO THE FACULTY OF ENGINEERING UNIVERSITY OF MALAYA, IN PARTIAL FULFILMENT OF THE REQUIREMENTS FOR THE DEGREE OF MASTER OF POWER SYSTEM ENGINEERING

2019

UNIVERSITY OF MALAYA

ORIGINAL LITERARY WORK DECLARATION

Name of Candidate: Chan Kok Wai

Matric No: KQI160020

Name of Degree: Master of Power System Engineering

Title of Research Report ("this Work"): An Investigation of Grading Margin Violation in Coordinating Overcurrent Relay

Field of Study: Power System Protection

I do solemnly and sincerely declare that:

(1) I am the sole author/writer of this Work;
(2) This Work is original;
(3) Any use of any work in which copyright exists was done by way of fair dealing and for permitted purposes and any excerpt or extract from, or reference to or reproduction of any copyright work has been disclosed expressly and sufficiently and the title of the Work and its authorship have been acknowledged in this Work;
(4) I do not have any actual knowledge nor do I ought reasonably to know that the making of this work constitutes an infringement of any copyright work;
(5) I hereby assign all and every rights in the copyright to this Work to the University of Malaya ("UM"), who henceforth shall be owner of the copyright in this Work and that any reproduction or use in any form or by any means whatsoever is prohibited without the written consent of UM having been first had and obtained;
(6) I am fully aware that if in the course of making this Work I have infringed any copyright whether intentionally or otherwise, I may be subject to legal action or any other action as may be determined by UM.

Candidate's Signature Date:

Subscribed and solemnly declared before,

Witness's Signature Date:

Name:

Designation:

ABSTRACT

In a radial distribution network, overcurrent protection is commonly used to protect against faults. The overcurrent protection is achievable with the installation of a circuit breaker and an overcurrent relay with an associated current transformer at the infeed of each feeder. The overcurrent relay protection grading scheme is widely being discussed among the power system protection engineers to ensure fast yet reliable fault detection and clearance. There are currently two overcurrent relay grading methods that have been practiced in the industry to provide discrimination between the main and backup relay. One of the relay grading methods is proposed by (Hall Stephens, 1998) and the other grading method is proposed by (Ravindranath & Chander, 1977). In this research work, the two different relay grading methods practiced in the industry are presented and successfully applied for the grading of the main-backup relay pairs. The grading margin for the two methods of overcurrent relay grading methods has been investigated under the various power system dynamic scenarios such as change in load size, fault resistance, fault location, and distribution cable length. Through the short-circuit simulation in Simulink under the various power system dynamic scenarios, it was found that when using Hall's Method to grade the relays, there are 28 cases (17.28%) in which the grading margin is below 0.3s indicating that relay grading margin is jeopardized. In contrast, when using Ravindranath's Method to grade the relays, all calculated grading margin are 0.3 seconds and above for all the 162 cases (100%), which proved that the integrity of grading margin is secured. The theoretical findings through the simulation has been validated through real-time Hardware-in-Loop (HIL) experiment using OPAL-RT simulator. Through the HIL experiment, the generated results are similar to the results obtained from the Simulink simulation for all the main and backup relay pairs, R3-R2 and R2-R1 which are tabled in Appendix A.

ABSTRAK

Dalam sistem radial, perlindungan arus lebihan biasanya digunakan untuk melindungi litar daripada arus litar pintas. Perlindungan arus lebihan boleh dicapai dengan pemasangan pemutus litar dan geganti arus lebihan dengan alatubah arus yang bersesuaian pada *infeed* setiap penyuap 3-fasa. Skema koordinasi perlindungan geganti arus lebihan sentiasa dibincangkan di kalangan jurutera perlindungan sistem kuasa untuk memastikan pengesanan dan pelepasan kesalahan yang cepat dan boleh dipercayai. Kini, terdapat dua kaedah penggredan untuk geganti arus lebihan yang telah diamalkan dalam industri untuk memastikan terdapat diskriminasi secukupnya antara geganti utama dan geganti sandaran. Salah satu daripada kaedah penggredan aliran arus lebihan telah dicadangkan oleh (Hall Stephens, 1998) dan kaedah kedua pula dicadangkan oleh (Ravindranath & Chander, 1977). Dalam penyelidikan ini, dua kaedah yang berbeza penggredan aliran arus lebihan yang diamalkan dalam industri ini telah dibentangkan dan berjaya digunakan untuk penyelarasan pasangan geganti utama-sandaran. Perbezaan tempoh masa operasi antara geganti utama dan geganti sandaran setelah digredkan dengan menggunakan kedua-dua kaedah penggredan geganti arus lebihan telah disiasat di bawah pelbagai senario sistem dinamik kuasa seperti perubahan saiz beban, rintangan kesalahan arus rosak, lokasi kesalahan arus rosak, dan kepanjangan kabel pengedaran. Melalui simulasi litar pintas di Simulink di bawah pelbagai senario sistem dinamik kuasa, didapati bahawa terdapat kemungkinan sebanyak 28 kes iaitu bersamaan dengan 17.28% kemungkinan di mana perbezaan tempoh masa operasi antara geganti utama dan geganti sandaran setelah digredkan dengan menggunakan Kaedah Hall adalah kurang dari 0.3 saat. Sekiranya menggunakan Kaedah Ravindranath untuk menggredkan pasangan geganti utama-sandaran pula, perbezaan tempoh masa operasi antara geganti utama dan geganti sandaran adalah 0.3 saat dan ke atas. Penemuan daripada simulasi telah disahkan melalui eksperimen Perkakasan-dalam-Loop (HIL) masa nyata menggunakan simulator

OPAL-RT. Hasil penemuan daripada eksperimen HIL ini adalah konsisten dengan hasil penemuan yang diperoleh daripada simulasi Simulink untuk kesemua pasangan geganti utama-sandaran, R3-R2 dan R2-R1 yang dibentangkan di Lampiran A.

ACKNOWLEDGMENTS

Firstly, I would like to express my sincere appreciation to Dr. Tan Chia Kwang, for his patience and encouragement during this research. His insightful comments and thought-provoking questions at various stages in this research kept the me inspired and enabled me to develop a profound understanding in this field of study.

The next person that I would like to express my thanks is Ms Jorinda, a doctoral student from University of Malaya Power Energy Dedicated Advanced Centre (UMPEDAC). She has been so willing to guide me especially in operating the OPAL-RT simulator.

A heartfelt gratitude to my parents, Mr. Chan Lee Fook and Madam Lim Kim Thai, for their unconditional love and support throughout the time spent preparing this research report. They have always been a pillar of strength to me.

Financial support during the Master of Engineering studies, provided by the Ministry of Higher Education (MOHE) Malaysia through MyBrain15 sponsorship is gratefully acknowledged.

TABLE OF CONTENTS

LIST OF FIGURES

LIST OF TABLES

LIST OF SYMBOLS AND ABBREVIATIONS

A	:	Ampere (amp)
AL	:	Aluminium
CB	:	Circuit breaker
CT	:	Current transformer
d_F	:	Fault location
GM	:	Grading Margin
$GM_{R2-R1(Hall's\ Method)}$	:	Time interval between the operation of relay R1 and relay R2 for the recorded fault current when the relay pair is graded using Hall's Method
$GM_{R2-R1(Ravindranath's\ Method)}$	:	Time interval between the operation of relay R1 and relay R2 for the recorded fault current when the relay pair is graded using Ravindranath's Method
HIL	:	Hardware-in-loop
Hz	:	hertz
IDMT	:	Inverse definite minimum time
IEEE	:	Institute of Electrical and Electronics Engineers
Is	:	Pick-up current of the relay
kA	:	kilo-Amperes
km	:	kilometres
kV	:	kilo-Volts
L	:	Load size

l	:	Cable length
mm	:	millimeter
MV	:	Medium Voltage
MVA	:	Mega-Volt-Amperes
MVAr	:	Mega-Volt-Amperes-reactive
MW	:	MegaWatts
OC	:	Overcurrent
P	:	Active power, in watts
ph	:	Phases of an electrical circuit
PMU	:	Transmission Main Intake (Pencawang Masuk Utama)
PPU	:	Main Distribution Substation (Pencawang Pembahagian Utama)
PSM	:	Plug setting multiplier
p.u.	:	per unit
Q	:	Reactive power, in volt-amperes-reactive
R	:	Electrical resistance
R_F	:	Fault resistance
RMS	:	Root mean square
ROT	:	Relay operating time
ROT_{R1}	:	Actual relay operating time of relay R1 for recorded fault current
s	:	seconds
S	:	Apparent power, in volt-amperes
SI	:	Standard inverse
T	:	Time, in seconds

T_{gm}	:	Time-grading margin allowance
TNB	:	Tenaga Nasional Berhad
TMS	:	Time multiplier setting
X	:	Electrical reactance
XLPE	:	Cross-linked polyethylene
Z	:	Electrical impedance
Ω	:	Ohms

LIST OF APPENDICES

CHAPTER 1: INTRODUCTION

1.1 Research Background

Power system protection is essential to ensuring reliability in electricity supply. The occurrence of a fault in the electrical network is unavoidable. These faults could be a single line-to-ground fault, line-to-line fault, double line-to-ground fault, or even a balanced three-phase fault (Grainger & Stevenson, 1994). Therefore, it is essential for the protection relay closest to the fault to detect and signal the circuit breaker to isolate the fault as fast as possible. This will minimize the number of customers affected by the fault.

Among the many protection relays used in the electrical network include the distance relay, differential relay, overcurrent relay and earth fault relay. In a radial distribution network, overcurrent protection is commonly used to protect against faults. The overcurrent protection is achievable with the installation of a circuit breaker and an overcurrent relay with an associated current transformer at the infeed of each feeder. It is essential that the operation of the overcurrent relays be appropriately coordinated to obtain proper discrimination when protecting a radial feeder with several circuit breakers and protection relays.

There has been a discussion among the power system protection engineers in the industry on the overcurrent protection grading scheme which fulfills the speed and reliability in fault detection and clearance. There are currently two overcurrent relay grading methods that have been practiced in the industry to provide discrimination between the main and backup relay. Therefore, there is a need to further investigate these two relay grading methods.

1.2 Research Objectives

The objectives of this research work are:

(a) To apply the two different methods of overcurrent relay grading practiced in the industry.

(b) To investigate the main-backup relays grading margin for the two methods of overcurrent relay grading under the various power system dynamic scenarios.

(c) To validate the theoretical findings through real-time Hardware-in-the-Loop (HIL) experiment using OPAL-RT simulator.

1.3 Scope and Limitation

The scopes and limitations of the study are:

(a) To consider only the 33kV radial distribution network in this study which is modelled using Simulink software.

(b) To consider only overcurrent protection feature of the relay.

(c) Only three-phase faults are simulated.

1.4 Outline of the Research Report

The research report is organized in five chapters. The first chapter gives a brief introduction to the research work. The topics covered include research background, objectives as well as the research scopes and limitations.

Chapter 2 mainly presents the comprehensive studies of literature reviews and theories which are important in developing a preliminary concept and project objectives. The reviewed topics cover the radial distribution network architecture, fundamental principles of overcurrent protection, characteristics of overcurrent protection, relay time grading margin, and methods of overcurrent relay grading practiced in the industry.

The methodology is described in Chapter 3. This chapter will explain the procedures in developing and modelling the test system in Simulink for short circuit study. Two different methods to grade the overcurrent relays for the radial distribution network as practiced in the industry is also presented step-by-step in this chapter. The methodologies then cover the fault simulations under varied dynamic power scenarios to record the fault current seen by the relay. The chapter continues with identifying the grading margin for each of the main-backup relay pairs for both methods of relay grading. Validation of the simulation results through real-time HIL experiment using OPAL-RT simulator is also explained in this chapter.

In Chapter 4, the results for one selected experiment condition are presented and discussed. In the first part of Chapter 4, the maximum short-circuit current at respective busses obtained from the short circuit study is recorded and tabled. The time multiplier setting (TMS) and plug setting multiplier (PSM) of the main and backup relays calculated from the relay grading using the two different methods are also tabled in this chapter. The grading margin for each of the main-backup relay pairs for both methods of relay grading is presented. In the second part, the theoretical findings are validated through HIL experiment using the OPAL-RT simulator.

Lastly, Chapter 5 presents the conclusion and recommendations for future work.

CHAPTER 2: LITERATURE REVIEW

2.1 Introduction

This project initiates the introduction of the concepts of radial distribution network architecture and overview of overcurrent protection such as the IDMT relay characteristics, relay setting current, and the relay grading margin. After establishing a sound concept on the overview of overcurrent protection, it presents a detailed literature review on the two relay grading methods practiced in the industry.

2.2 Distribution Network Architecture

There are three main distribution network architectures, which are the radial network, ring network, and mesh network architectures. The paper (Prakash, Lallu, Islam, & Mamun, 2016) elaborates on the review of each network topology regarding application, advantages, and disadvantages of each network architecture.

Most of the distribution systems use radial feeder network topology (Sallam & Malik, 2011). The radial network topology, in comparison to the ring network and mesh network, is the simplest and least expensive to construct. There is more likelihood of power outages when a fault occurs in the distribution feeder. One or more loads will be interrupted until the fault is located and cleared.

Figure 2.1 depicts the radial distribution system with 33 buses. IEEE has also developed other three-phase radial networks to be used for power system studies, include 13-bus feeder, 34-bus feeder, 37-bus feeder, and 123-bus feeder (Kersting, 2001). Each of these systems represents reduced-order models of an actual distribution network.

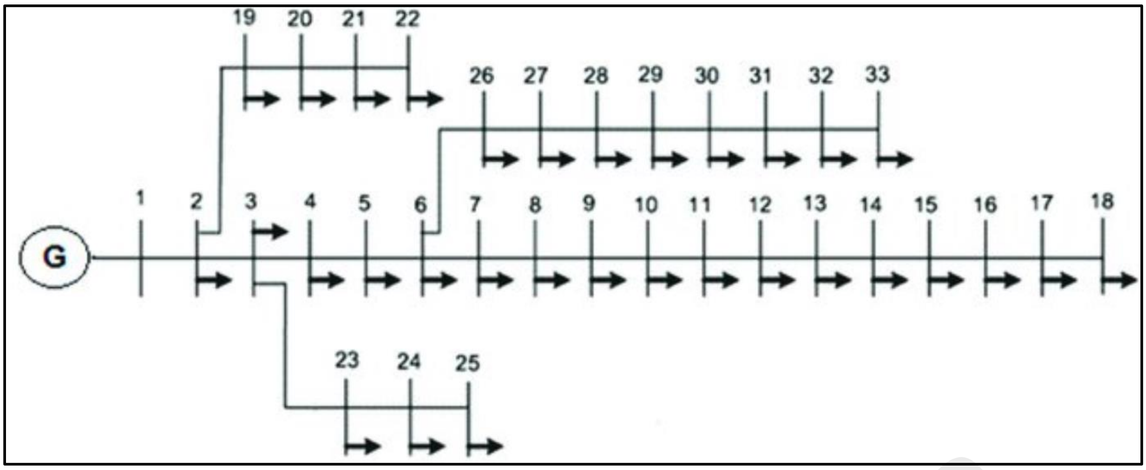

Figure 2.1: IEEE 33-Bus Radial Test Feeder.

2.3 Fundamental Principle of Overcurrent Relay

2.3.1 Plug Setting Multiplier (PSM)

Plug setting multiplier is defined as the ratio of fault current to the relay setting current (Paithankar & Bhide, 2011). The plug setting multiplier allows tapping in the electronic relays to give discrete settings in terms of the relay setting current. The typical settings for the PSM would be 0.05, 0.75, 1.00, 1.25, and 1.50, 1.75 and 2.00 of the rated relay operating time.

2.3.2 Time Multiplier Setting (TMS)

Each relay has a continuously variable TMS to change the operating time, at a specified plug setting, over certain specified limits (van C. Warrington, 1977). The range of variation is on the relay make. Using Time Multiplier Setting alongwith the Plug Setting Multiplier, the time-overcurrent curves of the relays can be plotted to verify that proper time discrimination has been provided for the main-backup relay pairs for their operation.

2.4 Characteristics of IDMT Overcurrent Relays

2.4.1 Standard IDMT Relay Characteristics

The current or time tripping characteristics of IDMT relays may need to be changed according to the functioning time needed and the characteristics of other relay elements used in the network (Mason, 1956). Based on the IEC 60255, the standard characteristic of the relay includes standard inverse characteristic (SI), very inverse characteristic (VI), extremely inverse characteristic (EI), and long-time standby earth fault characteristic. These relay characteristics curves are expressed mathematically in Table 2.1. The curves based on a common setting current (Is) and TMS of 1 second are shown in Figure 2.2.

Table 2.1: Standard Relay Characteristic Equations

Relay Characteristic	**Equation (IEC 60255)**
Standard Inverse	$t = TMS \times \frac{0.14}{\left(\frac{I}{I_s}\right)^{0.02} - 1}$
Very Inverse	$t = TMS \times \frac{13.5}{\left(\frac{I}{I_s}\right) - 1}$
Extremely Inverse	$t = TMS \times \frac{80}{\left(\frac{I}{I_s}\right)^{2} - 1}$
Long-time Inverse	$t = TMS \times \frac{120}{\left(\frac{I}{I_s}\right) - 1}$

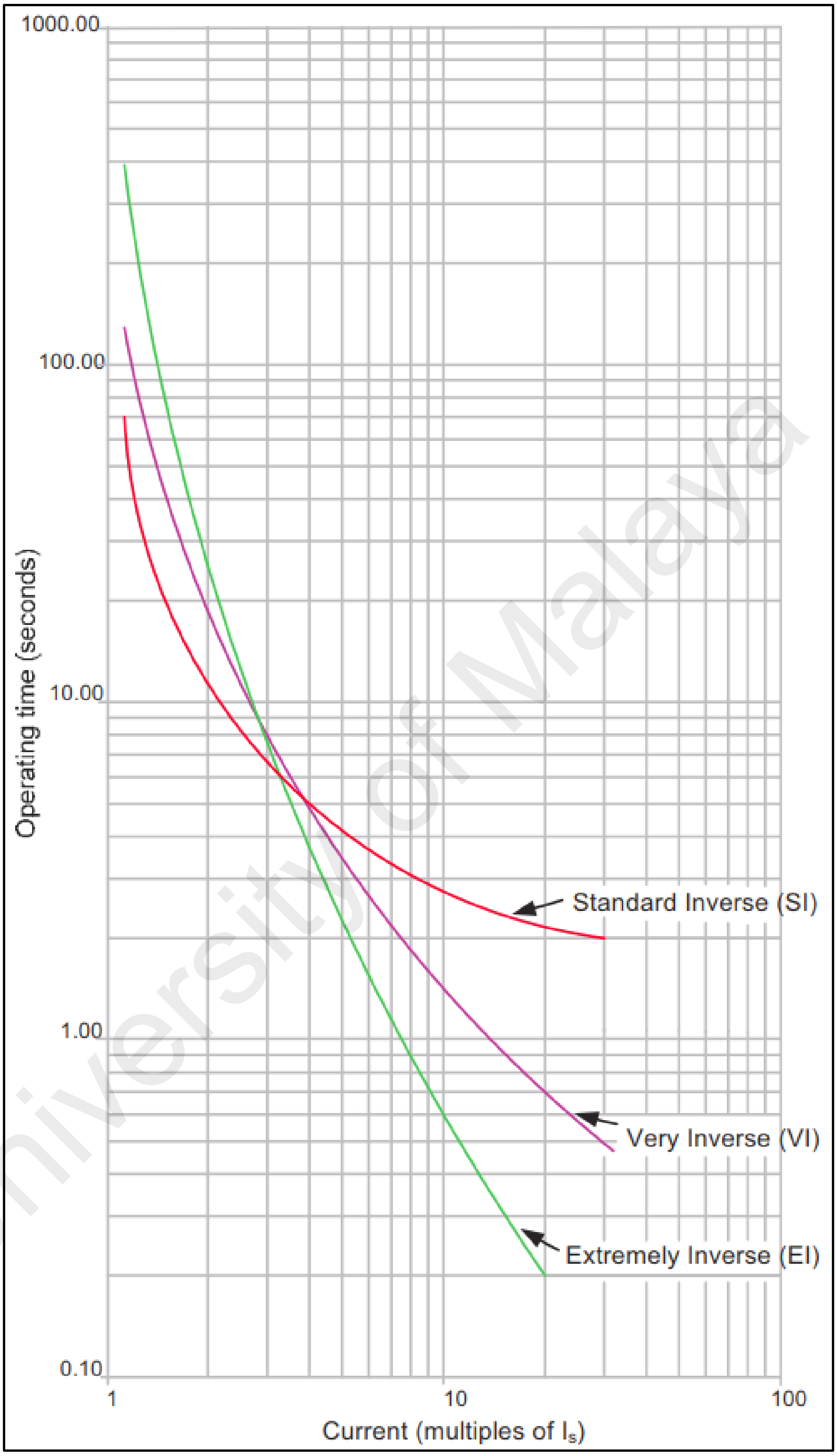

Figure 2.2: Standard IDMT relay characteristics based on IEC 60255.

2.4.1.1 Standard Inverse

Even though Figure 2.2 only presents discrete values of TMS, continuous settings may be feasible. For other relay types aside from electromechanical protection relay, the protection setting steps may be so small as to efficiently give continuous adjustment. Almost all overcurrent protection relays are equipped with high-set instantaneous devices. In most situations, the use of Standard Inverse (SI) protection curve is satisfactory. However, if acceptable grading cannot be accomplished, either Very Inverse (VI) or Extremely Inverse (EI) protection curve can be used. When digital or numerical relays are used, other characteristics may be selected, including the possibility of user-defined protection curves.

2.5 Relay Current Setting

An overcurrent protection relay has a minimum relay current setting. The current setting has to be selected so that the protection relay does not trip for the maximum load current in the circuit being protected, but does trip for a current same or higher to the minimum anticipated short-circuit current (Webster & Das, 2017). The relay current setting is chosen to be above the maximum short time rated current of the protected network.

2.6 Relay Time Grading Margin

Grading margin (GM) refers to the time duration that is to be allowed between the operation of two relays (one main relay and another backup relay) to achieve proper discrimination between them. If a grading margin is too little, both the relays will operate for a short circuit at same time. As such, it will be difficult to locate the fault and isolate it. Failure in doing so has led to more customers affected by the unnecessary loss of electricity supply.

The grading margin mainly depends on the fault current interrupting time of the circuit breaker, relay overshoot time, and CT and relay errors during the relay operation. Figure 2.3 shows that the relay grading margin is equivalent to the sum of time taken by the relay and current transformer (CT) error (denoted by 'C1' and 'C2'), circuit breaker breaking time (denoted by 'A'), relay overshoot time (denoted by 'B'), and safety margin (denoted by 'D').

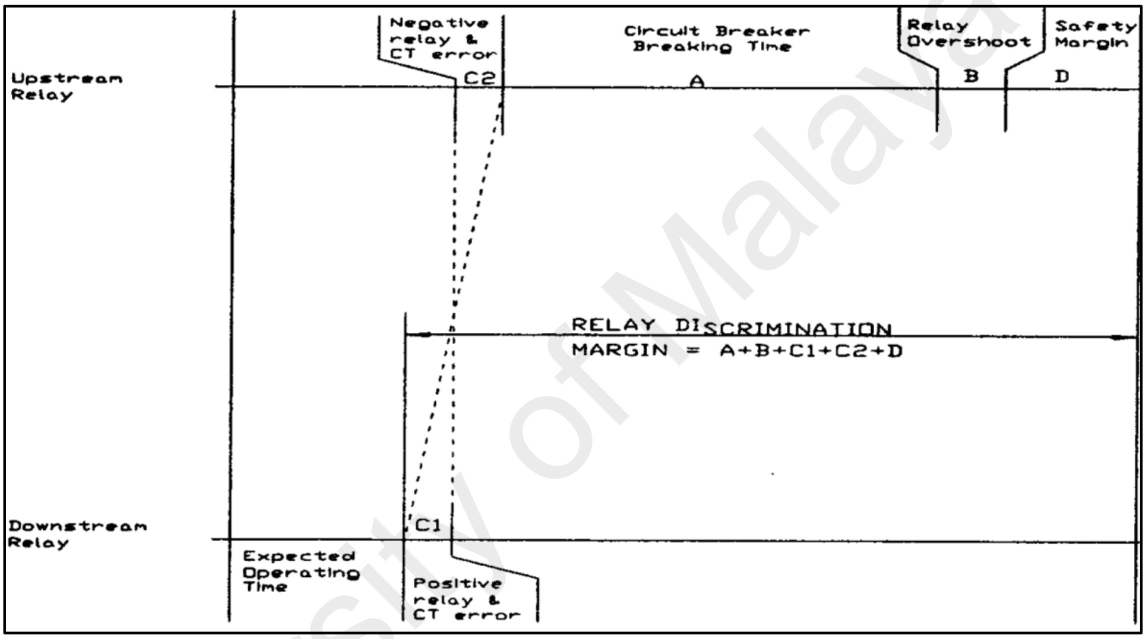

Figure 2.3: Relay Grading Margin dependent on Relay and CT errors and Safety Margin.

2.6.1 Circuit Breaker Interrupting Time

Circuit breaker interrupting, or the breaking time is the time taken to completely interrup the fault current before the coordinated relay has stopped energizing (IEEE, 1998, 2001). The time taken is dependent on the circuit breaker technology and the amount of fault current to be interrupted. Figure 2.4 shows how the relay grading margin is dependent on the relay reset time. Relay reset time is comprised of the relay interrupting time (or breaking time) and relay overshoot time. Relay interrupting time is equivalent to the sum of the relay operating time and relay arcing time. Relay operating time is from the time relay operates which is at time t2 until circuit breaker contact separates at time t3. The relay arcing time begins from the moment the circuit breaker contact separates at time t3 until the arc has been cleared at time t4.

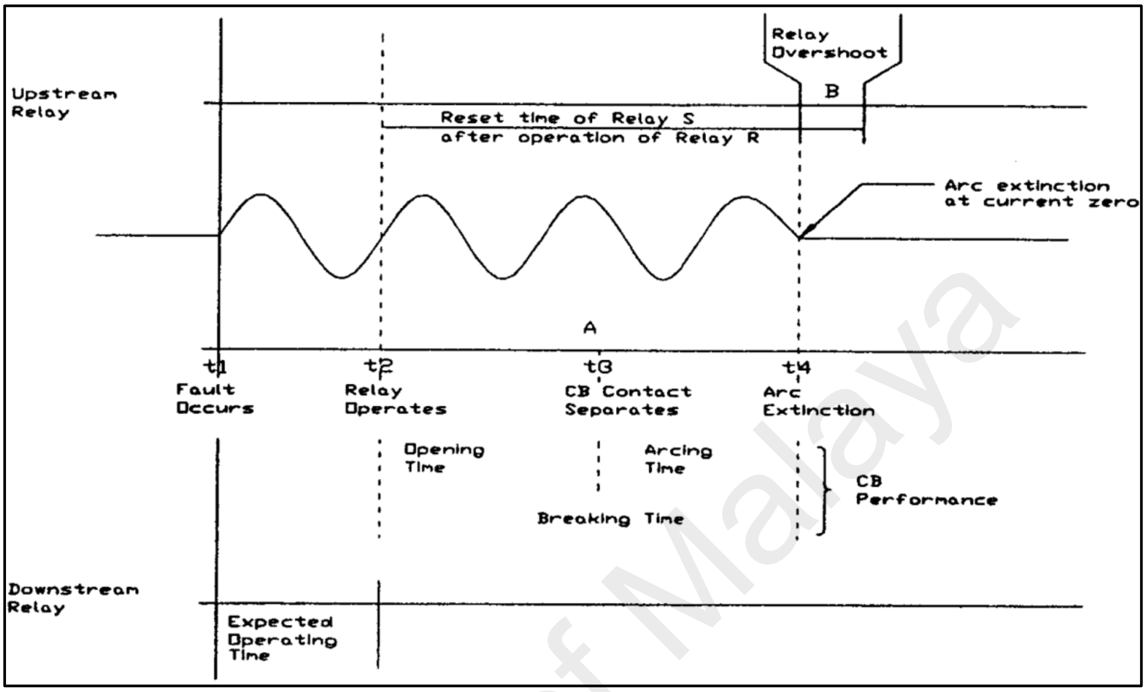

Figure 2.4: Relay Grading Margin dependent on Relay Reset Time.

2.6.2 Relay Overshoot

As illustrated in Figure 2.4, when the relay is de-energized at time t4 after arc extinction at current zero, the ripping of the relay may continue for a little longer (denoted as 'B') until any stored energy has depleted (Association & Engineers, 1995). Relay design is aimed at minimizing and absorbing these energies, but some allowance is typically required. The overshoot time is defined as the difference between the relay tripping time at a defined value of input current and the maximum duration of input current, which when abruptly reduced below the relay operating level, is insufficient to cause relay operation (Blackburn & Domin, 2014)

.

2.6.3 Relay and CT Errors

All relays have errors in their timing in comparison to the ideal characteristic as specified in IEC 60255 (Prévé, 2013). The maximum timing error must be considered when coordinating the main-backup relay pairs.

Current transformers have phase and ratio errors due to the excitation current required to magnetize their cores. As a result, the CT secondary current is not identically scaled to the primary current. This leads to errors in the operation of relays, particularly in the operation time.

In Figure 2.3, the positive CT and relay error by the main relay is denoted by 'C1' whereas the negative CT and relay error by the backup relay is denoted by 'C2'. These 'C1' and 'C2' time duration will therefore needs to be considered when calculating the grading margin for the main-backup relay pairs.

2.6.4 Safety Margin

Apart from the allowances for the CB breaking time, relay overshoot time, and CT and relay errors, additional safety margin is provided to ensure that the relay does not maloperate.

2.6.5 Recommended Relay-to-Relay Grading Margin

The total interval needed to cover circuit breaker clearing time, relay timing error, overshoot and CT errors, is dependent on the tripping speed of the circuit breakers and the relay performance. In the past, the typical grading margin proposed was 0.5 seconds. With recent advancements in circuit breaker and relay technologies, there has been an improvement in the grading margin. A grading margin of 0.4 seconds is practical , due to the contribution from the faster CB interrupting time and relay overshoot time.

The Table 2.2 tabulates typical coordinating time interval between overcurrent relays for different technologies, which are electromechanical relay, static relay, digital relay, and numerical relay.

Table 2.2: Common protection relay grading margin – standard IDMT relays (Alstom, 2011).

	Relay protection type			
	Electromechanical	Static	Digital	Numerical
Typical basic timing error (%)	7.5	5	5	5
Overshoot time (s)	0.05	0.03	0.02	0.02
Safety margin (s)	0.1	0.05	0.03	0.03
Typical overall grading margin – relay-to-relay (s)	0.4	0.35	0.3	0.3

2.7 Overcurrent Relay Grading Methods

(Hall Stephens, 1998) has proposed to consider the maximum short circuit at the downstream busbar when calculating for the time multiplier setting and relay operating time. The left column of Figure 2.5 shows the proposed relay grading method by (Hall Stephens, 1998). Busbar 1 is the upstream busbar whereas Busbar 2 is the downstream busbar. From this Figure 2.5, the maximum short-circuit current obtained at Busbar 2 during short circuit study is to be collected and used to grade the R1 relay.

(Ravindranath & Chander, 1977) has proposed to consider the maximum short circuit at the upstream busbar when calculating the time multiplier setting and relay operating time. The right column of Figure 2.5 shows the proposed relay grading method by (Ravindranath & Chander, 1977). Busbar 1 is the upstream busbar whereas Busbar 2 is the downstream busbar. From this Figure 2.5, the maximum short-circuit current obtained at Busbar 1 during short circuit study is to be collected and used to grade the R1 relay.

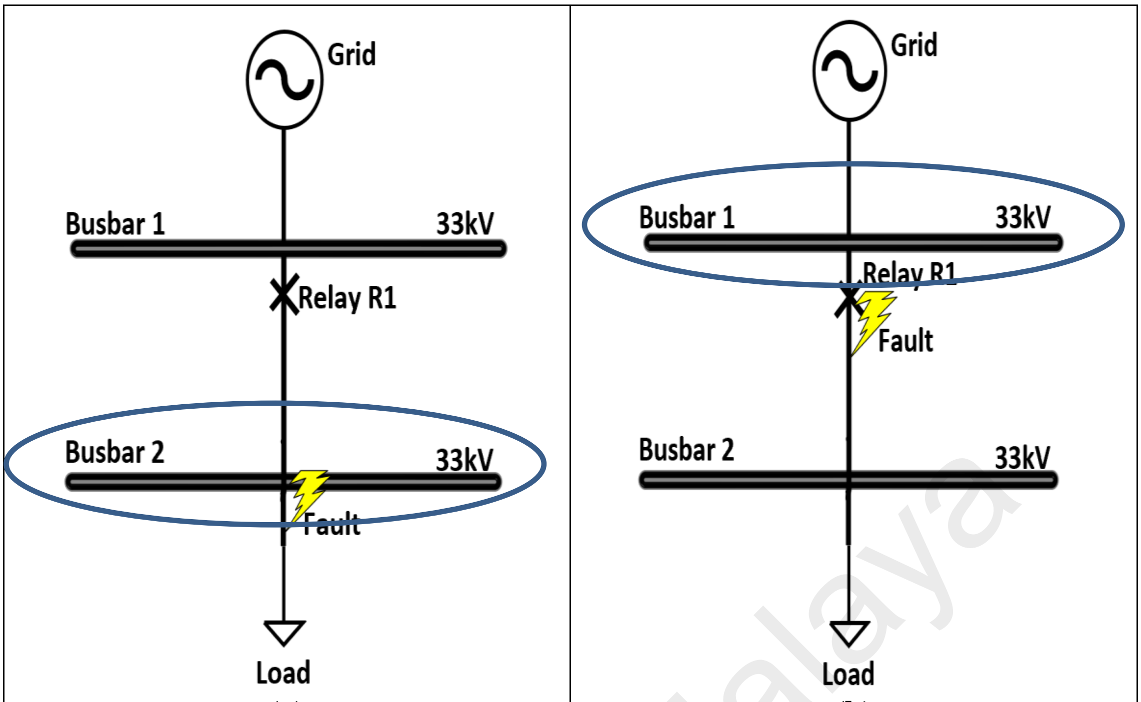

(a)	(b)
Example of relay grading using Hall's Method: $ROT_{(R1)} = TMS_{(R1)} \times \frac{0.14}{\left(\frac{I_{f\,(Busbar\ 2)}}{I_s}\right)^{0.02} - 1}$	**Example of relay grading using Ravindranath's Method:** $ROT_{(R1)} = TMS_{(R1)} \times \frac{0.14}{\left(\frac{I_{f\,(Busbar\ 1)}}{I_s}\right)^{0.02} - 1}$

Figure 2.5: Comparison between relay grading method proposed by (a) (Hall Stephens, 1998) and (b) (Ravindranath & Chander, 1977)

2.8 Summary

The principle of the overcurrent protection which is the plug setting multiplier (PMS) and time multiplier setting (TMS) along with the standard characteristics of the overcurrent relay has been covered in this chapter. The two methods of the relay grading currently practiced in the industry which is Hall's Method and Ravindranath's Method have also been presented. Differences in terms of calculating the relay operating time between these two grading methods have been highlighted.

CHAPTER 3: RESEARCH METHODOLOGY

3.1 Introduction

This research work presents the grading method for overcurrent protection relays in a radial 33kV distribution network. The chapter begins with the configuration of the 33kV medium voltage distribution network. Then the modelling of the distribution network in the simulation tool will be elaborated. Short circuit analysis of the network will be further explained. Step-by-step procedure for grading the overcurrent protection relays are then presented. Finally, the methodology for hardware implementation will be discussed.

3.2 System Model Description

The 33kV medium voltage distribution network used in this research work is illustrated in Figure 3.1. The network begins from PMU (Transmission Main Intake) which houses a single 132/33kV power transformer. In this network, there are four PPUs (Main Distribution Substation), which are denoted as PPU 1, PPU 2, PPU 3, and PPU 4. Power is transmitted from the 132kV PMU to the PPUs along the radial feeder via the 90MVA 132/33kV transformer. Each of the PPUs is connected to a load. These loads represent different groups of consumers comprising of industrial, residential and commercial. Since this project is limited to only 33kV network, the 33/11kV 30MVA distribution transformers and fuses feeding the loads at the PPUs are omitted. Only the circuit breakers and the current transformers are shown in the single line diagram.

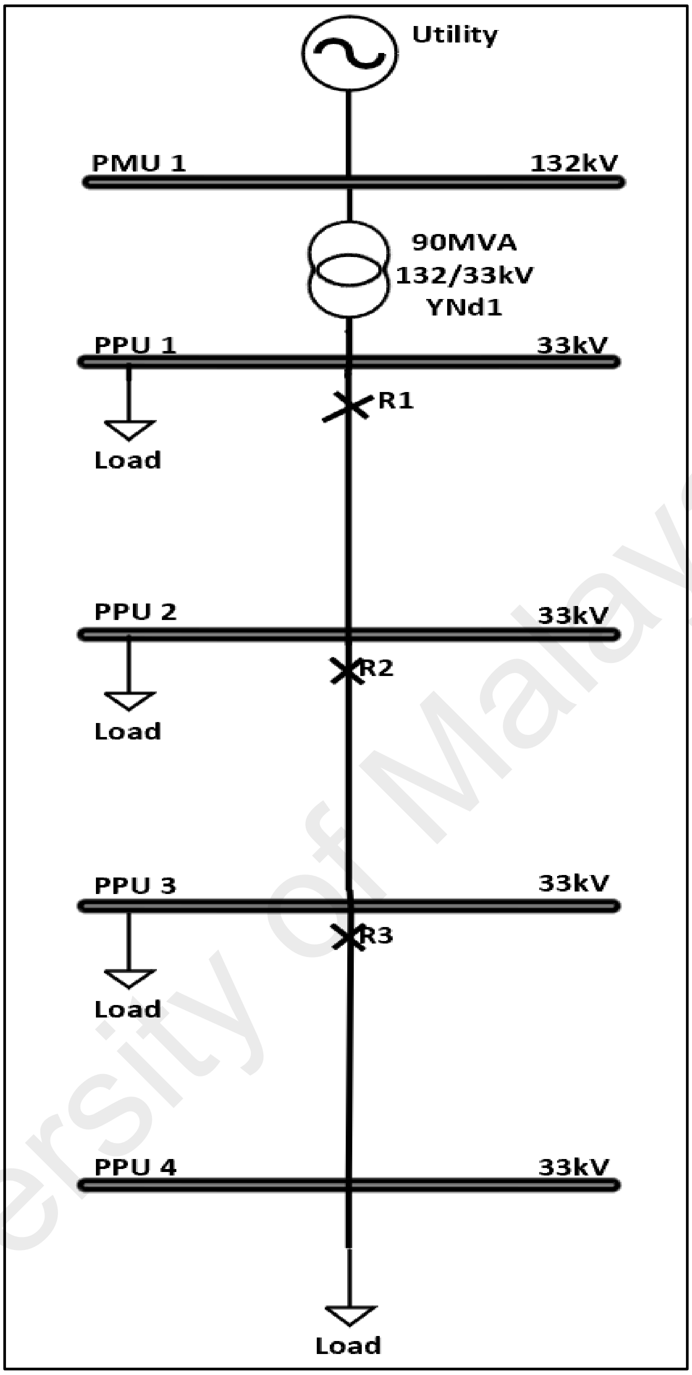

Figure 3.1: System configuration for radial MV distribution network.

3.3 Distribution System Modelling in Simulink

The 33kV radial test feeder network is modelled in Simulink, as shown in Figure 3.2. For modelling purposes, some simplifications have been made to the electrical balance of plant that is not expected to have a material impact on the study results.

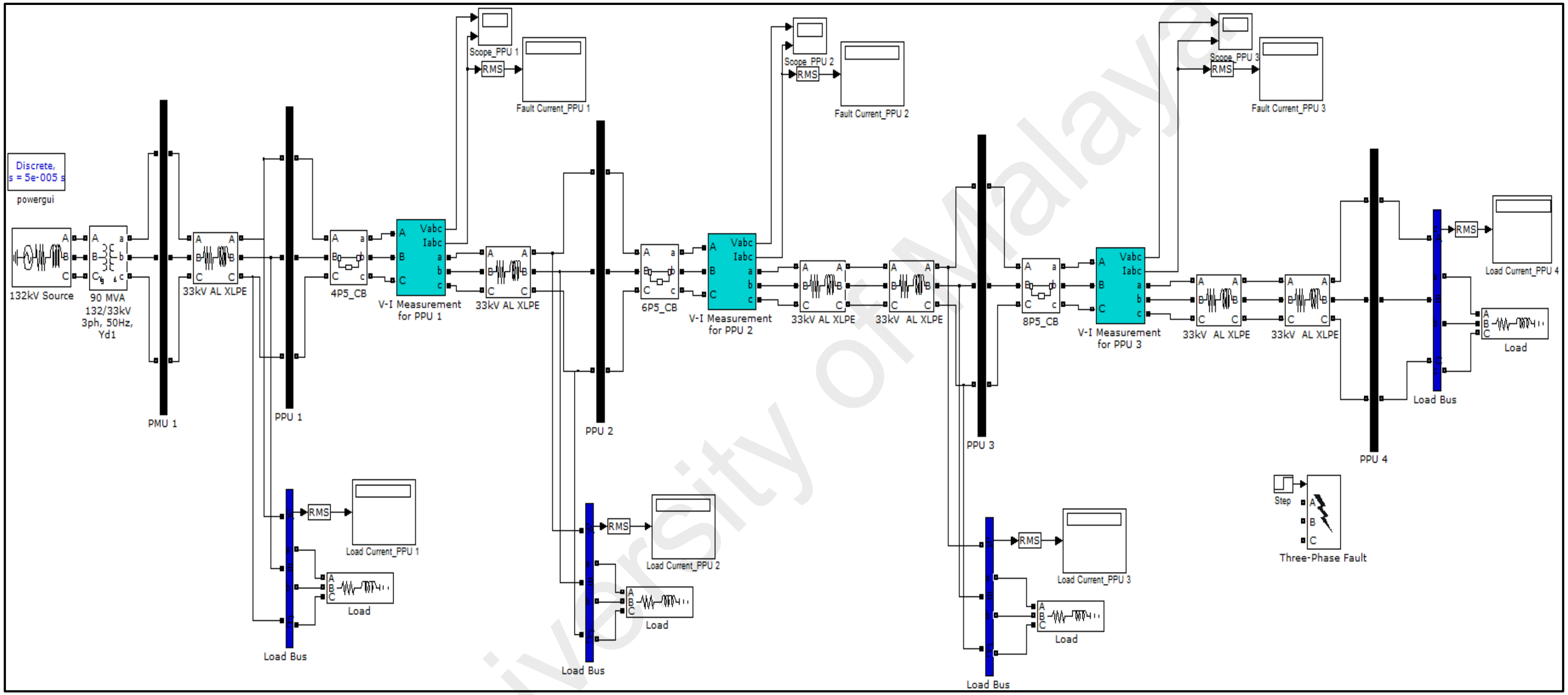

Figure 3.2: Modelling of the test system in Simulink.

3.3.1 Utility Grid Modelling

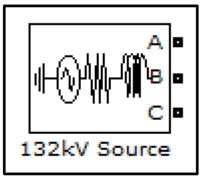

Figure 3.3: Utility Grid Model in Simulink.

The utility supply is modelled using the model in Figure 3.3, as a three-phase wye-connected voltage source in series with resistance and inductance values determined from the nominal system voltage, short circuit capacity, and X/R ratio, as shown in Table 3.1. The maximum short circuit current in the utility grid is set to 25kA, representing the actual short circuit current level at the 33kV system (Distribution, 2011). To set the maximum short circuit current rating to be 25kA, the 3-phase short circuit power at 132kV base voltage is calculated using Equation 3.1 – Equation 3.4 .

$$I_p = \frac{V_s}{V_p} I_s \quad (3.1)$$

$$I_p = \left(\frac{33kV}{132kV}\right) I_s = \left(\frac{1}{4}\right) I_s = \frac{25000A}{4} = 6250A \quad (3.2)$$

$$S = \sqrt{3} \times V_p \times I_p \quad (3.3)$$

$$S = \sqrt{3} \times 132kV \times 6250A = 1429MVA \quad (3.4)$$

Table 3. 1: Utility Data

Parameter	Value
Generator type	Swing
Internal connection	Yg
Nominal phase-to-phase voltage (RMS)	132 kV
Operating phase angle	0º
Frequency	50 Hz
3-phase short circuit power at a 132kV base voltage	1429 MVA
X/R ratio	20

3.3.2 Transformer Modelling

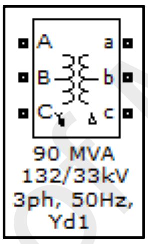

Figure 3.4: Three-phase Transformer Model in Simulink.

There is one single unit of transformer modelled in Simulink for this 33kV radial test feeder. The model is shown in Figure 3.4. The parameters of the transformer are listed in Table 3.2.

Table 3.2: 132/33kV Transformer Data

Parameter	Value
Rated MVA	90 MVA
Frequency	50 Hz
Rated voltage ratio (HV/LV)	132 kV / 33 kV
Vector group	YNd1
Impedance	13.5 %
Magnetization resistance	500 p.u.
Magnetization inductance	500 p.u.

3.3.3 Underground Cable Modelling

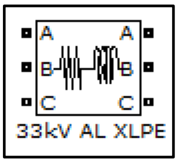

Figure 3.5: Cable model in Simulink.

The cable used for the distribution line between PMU 1 and PPU 1 is 630mm^2 XLPE underground cable. The size of XLPE underground cable used for distribution line between two units of PPUs (PPU 1 – PPU 2, PPU 2 – PPU 3, and PPU 3 – PPU 4) is 300mm^2. The model is shown in Figure 3.5. The parameters of the underground cables are listed in Table 3.3.

Table 3.3: 33kV Underground Distribution Line Data

Parameter	**Cable name**	
	XNHA27AA003	**XNHA32AA001**
Conductor	Aluminum	Aluminum
Conductor size	300 mm^2	630 mm^2
Insulation	XLPE	XLPE
Apparent power base	100 MVA	100 MVA
Rated voltage	33 kV	33 kV
Frequency	50 Hz	50 Hz
Positive Sequence Resistance	0.130 Ω/km	0.0629 Ω/km
Positive Sequence Reactance	0.106 Ω/km	0.107 Ω/km

For protection system analysis, it is usually the line series impedance that is required (Anderson, 1999). In a normal balanced operating state of an electrical system, only positive-sequence current will flow through. No negative-sequence or zero-sequence current is present. As such, since only the balanced three-phase fault is simulated in this research work, the zero-sequence impedance of the line segment can be omitted.

For the radial network topology, the relatively short lengths of MV distribution circuits are usually sufficient to be represented by a series impedance (Saadat, 2002). The capacitance is neglected unless in special cases which involve an earth fault on a network operating with an isolated neutral. In this special case, the phase-earth capacitances of short lines can be significant and need to be included (Lakervi & Holmes, 1995).This special case is not applicable to our study case.

3.3.4 Load Modelling

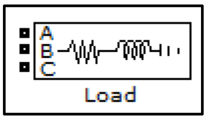

Figure 3.6: Load model in Simulink.

For load modelling, the essential parameters to be considered are total rated power and power factor which indicate how much the active power and reactive power that the load consumes. The model is shown in Figure 3.6. The parameters of the full 100% load are listed in Table 3.4.

Table 3.4: Load Data

Parameter	**Value**
Nominal phase-to-phase voltage	33 kV
Frequency	50 Hz
Power Factor	0.85
Load Type	Constant Impedance Z
Configuration	Wye, grounded
Active Power, P	25.5 MW
Inductive Reactive Power, Q_L	15.8 MVAr
Capacitive Reactive Power, Q_C	0 MVAr

3.3.5 Selection of Current Transformer (CT)

Selection of current transformers (CT) is essential before any placement of overcurrent protection relay and subsequent relay grading is carried out. A current transformer (CT) is an instrument transformer which is used to measure the load and fault current of the electrical distribution system. The primary current is stepped down to the ampere value acceptable by the protection relay.

The rated secondary current of all CTs is standardized at either 1A or 5A. Selection of secondary current rating of a CT is based on the location of CT and burden of the CT. Based on standard practice, indoor CTs (mounted in switchgear) shall have a 5A secondary current, whereas outdoor CTs (mounted at outdoor switchyard) shall have a 1A secondary current.

Modern protection and metering equipment have relatively low burdens. As such, the burdens in the cables are the predominant ones. By taking into consideration the cable burden which is represented by $P = I^2R$, a 1A circuit has a cable burden of 25 times lower VA in comparison to a 5A circuit. As a result, indoor CTs in recent years tend to have secondary windings of 1A as it results in a saving in CT size, weight, and cost as well as reduced losses in copper wires between the instrument and CT.

With the reasons discussed above, for this research work, the CT secondary current for the overcurrent protection is 1A. The CT primary current chosen must be higher than the maximum load current determined through the load flow analysis.

3.4 Short Circuit Analysis

Short circuit analysis of the network helps in estimating the magnitude of fault current flowing in the network when the fault occurs at any of the PPUs. It can be done through calculations or through simulations. In this research work, short circuit analysis of the

33kV radial distribution network is conducted through simulation in Simulink software. The Simulink model shown in Figure 3.2 will be used to perform the short circuit analysis. In Figure 3.7, the 132kV substation bus is represented by PMU 1 and the 33kV substation buses are represented by PPU 1, PPU 2, PPU 3, and PPU 4. The lines between the 33kV substations are denoted Line L1, Line L2, and Line L3. Faults applied at the respective 33kV bus are denoted as F1, F2, F3, and F4.

In this radial distribution network, the flow of current is unidirectional. Whenever fault happens, the current will flow from PMU 1 to respective fault location. The magnitude of fault current depends on the type of fault. In this research project, the three-phase fault is applied. The steps for short circuit analysis are as follows:

i. Apply a three-phase bolted fault at busbar of PPU 1. In Figure 3.7, this fault is represented by F1.
ii. Record the RMS current at the location where the fault is applied. The recorded short circuit current is denoted as $I_{sc_{max(i)}}$, where *i* represents the busbar number.
iii. Repeat steps (i) to (ii) for all other PPU busbars (PPU 2, PPU 3, and PPU 4). In Figure 3.7, it would be F2 simulated at busbar of PPU2, F3 simulated at busbar of PPU 3, and F4 simulated at busbar of PPU 4.

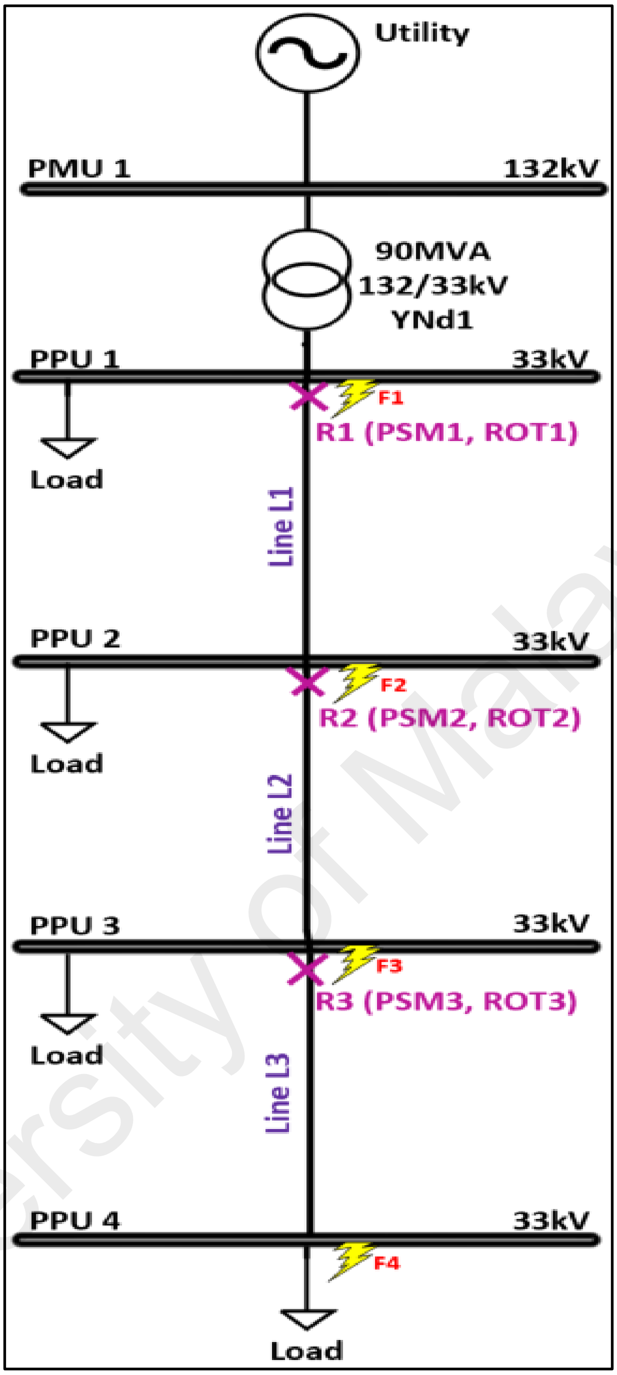

Figure 3.7: Network configuration for short circuit study.

Upon performing the steps above, the maximum short circuit current values of all the PPUs can be tabled. These maximum fault current values will be used for relay grading.

3.5 Perform Overcurrent Relay Grading

As discussed in Section 2.7, there are currently two methods of the relay grading currently practiced in the industry. One of the relay grading methods is proposed by (Hall Stephens, 1998) and the other relay grading method is proposed by (Ravindranath & Chander, 1977).

When performing grading for the main-backup relay pair, the relay mentioned first in the pair will be the main relay while the relay mentioned second in the pair will be the backup relay. For R3-R2 pair, relay R3 is the main relay, and relay R2 is the backup relay.

3.5.1 Hall's Method

This section presents a step-by-step procedure of the overcurrent relay grading in a radial distribution network configuration using Hall's Method. With reference to Figure 3.7, the flowchart in Figure 3.8 represents the procedures for overcurrent protection relay grading.

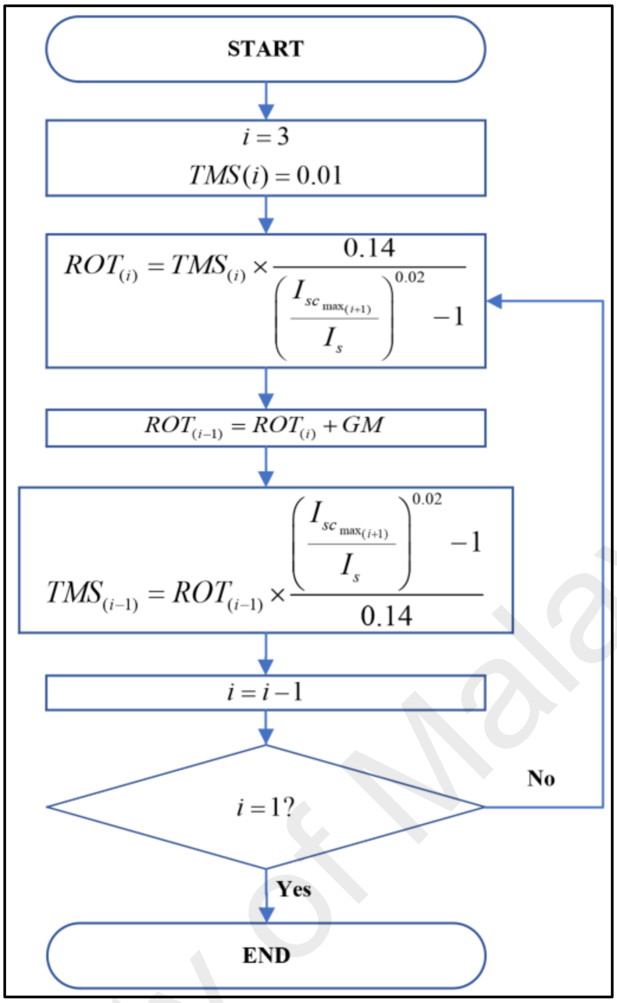

Figure 3.8: Flowchart of overcurrent protection relay grading using Hall's Method.

The stepwise TMS calculation method for relay grading using Hall's Method is explained below:

i. Initialize loop counter '*i*' to the value equivalent to the total number of relays in the radial test feeder. In this project, there are three relays present, denoted by R1, R2, and R3. Assign the lowest available TMS to the farthest relay R3. For example, TMS = 0.01 is assigned to R3.

ii. Calculate the Relay Operating Time (ROT) for the i^{th} relay by using standard inverse equation.

$$ROT_{(i)} = TMS_{(i)} \times \frac{0.14}{\left(\frac{I_{sc_{\max(i+1)}}}{I_s}\right)^{0.02} - 1} \tag{3.5}$$

In which TMS$_{(i)}$ represents the TMS assigned to the i^{th} relay. $I_{sc_{max(i+1)}}$ represents the maximum fault current at the $(i+1)^{th}$ PPU. With reference to Figure 3.7, TMS$_3$ represents the TMS assigned to R3. $I_{sc_{max_4}}$ represents the maximum fault current at busbar of PPU 4. This maximum fault current of the respective PPU is obtained in Section 3.4.

iii. Calculate the ROT for the $(i-1)^{th}$ relay which acts as a backup protection for the i^{th} relay. Grading margin (GM) of 0.3 seconds is used.

$$ROT_{(i-1)} = ROT_{(i)} + GM \tag{3.6}$$

iv. Compute the TMS of the $(i-1)^{th}$ relay (backup relay) using Equation 3.7.

$$TMS_{(i-1)} = ROT_{(i-1)} \times \frac{\left(\frac{I_{sc_{\max\ (i+1)}}}{I_s}\right)^{0.02} - 1}{0.14} \tag{3.7}$$

v. Perform grading for the next main-backup relay pair by reducing the counter, i as shown in Equation 3.8.

$$i = i - 1 \tag{3.8}$$

vi. Repeat steps (i) to (v) until the value of counter, i is equivalent to 1 at step (v).

Through steps (i) to (vi), the TMS for all the main and backup relay pairs, R3-R2 and R2-R1 will be calculated.

3.5.2 Ravindranath's Method

This section presents a step-by-step procedure of the overcurrent relay grading in a radial distribution network configuration using Ravindranath's Method. Figure 3.9 shows the flowchart representing the procedures for overcurrent protection relay grading.

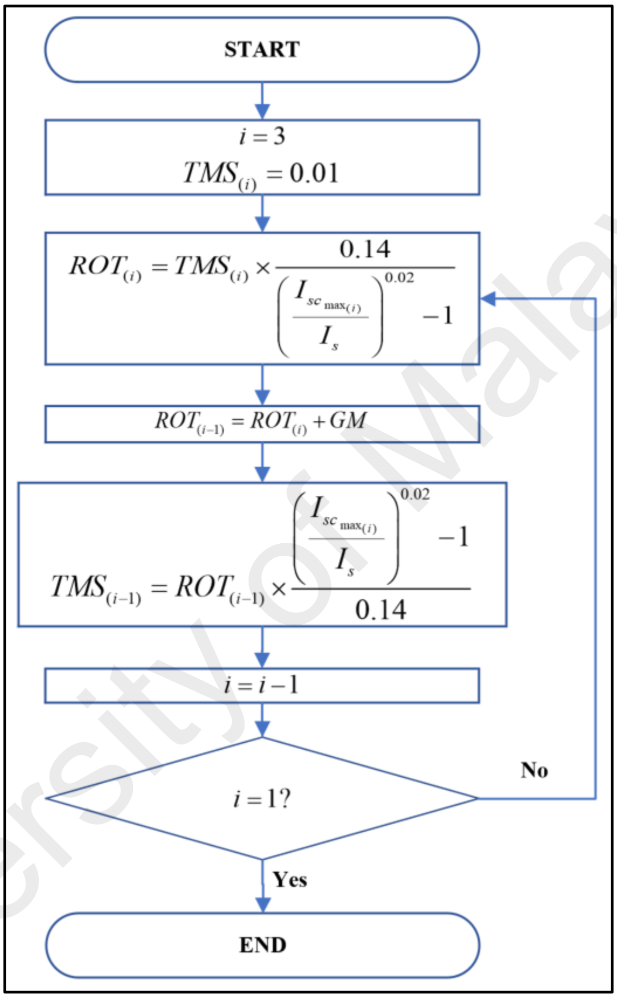

Figure 3.9: Flowchart of overcurrent protection relay grading using Ravindranath's Method.

The stepwise TMS calculation method for relay grading using Ravindranath's Method is explained below:

i. Initialize loop counter '*i*' to the value equivalent to the total number of relays in the radial test feeder. In this project, there are three relays present, denoted by R1, R2, and R3. Assign the lowest available TMS to the farthest relay R3. For example, TMS = 0.01 is assigned to R3.

ii. Calculate the Relay Operating Time (ROT) for the i^{th} relay by using standard inverse equation.

$$ROT_{(i)} = TMS_{(i)} \times \frac{0.14}{\left(\frac{I_{sc_{max\,(i)}}}{I_s}\right)^{0.02} - 1} \quad (3.9)$$

In which TMS$_{(i)}$ represents the TMS assigned to the i^{th} relay. $I_{sc_{max(i)}}$ represents the maximum fault current at the i^{th} PPU. With reference to Figure 3.7, TMS$_3$ represents the TMS assigned to R3. $I_{sc_{max_3}}$ represents the maximum short circuit current at PPU 3. This maximum fault current of the respective PPU is obtained in Section 3.4.

iii. Calculate the ROT for the $(i-1)^{th}$ relay which acts as a backup protection for the i^{th} relay. Grading margin (GM) of 0.3 seconds is used.

$$ROT_{(i-1)} = ROT_{(i)} + GM \quad (3.10)$$

iv. Compute the TMS of the $(i-1)^{th}$ relay (backup relay) using Equation 3.11.

$$TMS_{(i-1)} = ROT_{(i-1)} \times \frac{\left(\frac{I_{sc_{max\,(i)}}}{I_s}\right)^{0.02} - 1}{0.14} \quad (3.11)$$

v. Perform grading for the next main-backup relay pair by reducing the counter, i as shown in Equation 3.12.

$$i = i - 1 \quad (3.12)$$

vi. Repeat steps (i) to (v) until the value of counter, i is equivalent to 1 at step (v).

Through steps (i) to (vi), the TMS for all the main and backup relay pairs, R3 – R2 and R2 – R1 will be calculated.

3.6 Perform Short Circuit Simulations and Record Short Circuit Current under Various Power System Dynamic Scenarios

Upon the completion of relay grading using both relay grading methods as discussed in Section 3.5.1 and Section 3.5.2, a short-circuit simulation is conducted in Simulink. The Simulink model, with reference to Figure 3.10 is first initialized with the following preliminary parameters shown in Table 3.5.

Table 3.5: Initial Power System Dynamic Parameters for the Base Case

Parameters	**Base case value**
Fault location, d_F	0%
Fault resistance, R_F	0Ω
Load size	0%
Cable length, l	1km

Table 3.6 shows system parameters used to investigate the effects of the power system dynamics (fault location, fault resistance, load size, and cable length) on the grading margin of the relay pairs.

Table 3. 6: System parameters used to investigate effects of the power system dynamics on the grading margin of the relay pairs

Parameters	**Base case value**
Fault location, d_F	1) d_F = 0% 2) d_F = 50% 3) d_F = 100%
Fault resistance, R_F	1) R_F = 0Ω 2) R_F = 5Ω 3) R_F = 10Ω
Load size, L	1) L = 0% 2) L = 50% 3) L = 100%
Cable length, l	1) l = 1km 2) l = 3km 3) l = 5km

In this project, sensitivity analysis is adopted to investigate the effects of the power system dynamics (fault location, fault resistance, load size, and cable length) on the grading margin of the relay pairs. For this investigation, four case studies are developed.

a. Case Study 1

Case Study 1 is developed to investigate the effect of fault location on the grading margin for the relay pairs. In this case study, the simulation model shown in Figure 3.2 shall be free from the influence of fault resistance, load sizes, and cable lengths to ensure the results are solely reflecting the effect of fault resistance. With reference to Figure 3.10, as an example, for the relay pairs of R3-R2, the simulation is initiated with the fault resistance of 0% of the line L3 which is at busbar of PPU 3 and a constant value of fault resistance of 0Ω. The simulation is the repeated by changing the fault location to 50% and 100% of the line length.

b. Case Study 2

Case Study 2 is developed to investigate the effect of fault resistance on the grading margin for the relay pairs. This Case Study 2 still uses the same Simulink model configuration which was used in Case Study 1 and repeats the simulation steps in Case Study 1 by changing the fault resistance from 0Ω to 5Ω and 10Ω.

c. Case Study 3

Case Study 3 is developed to investigate the effect of load size on the grading margin for the relay pairs. This Case Study 3 still uses the same Simulink model configuration which was used in Case Study 2 and repeats the simulation steps in Case Study 2 by changing the load size from 0% to 50% and 100%.

d. Case Study 4

Case Study 4 is developed to investigate the effect of cable length on the grading margin for the relay pairs. This Case Study 4 still uses the same Simulink model configuration which was used in Case Study 3 and repeats the simulation steps in Case Study 3 by changing the cable length from 1km to 3km and 5km.

As referred to Table 3.6, the simulation steps for short circuit simulation to investigate the effects of the power system dynamics (fault location, fault resistance, load size, and cable length) on the grading margin of the relay pairs R3-R2 and R2-R1 are listed below:

i. A three-phase bolted fault is simulated at 0% of the line L3 which is at busbar of PPU 3.
ii. Record fault currents seen by both the main relay (represented by relay R3) and backup relay (represented by relay R2).

iii. Change fault location to 50% and 100% of the line length and repeat step (i) to (ii). This short circuit simulation study comprising of 3 fault location values is elaborated in Case Study 1.

iv. Change fault resistance from 0Ω to 10Ω, in step of 5Ω. Repeat step (i) to (iii). This short circuit simulation study comprising of 3 fault locations and 3 fault resistances is elaborated in Case Study 2.

v. Change load size from 0% to 100% load, in step of 50%. Repeat step (i) to (iv). This short circuit simulation study comprising of 3 fault locations, 3 fault resistances and 3 load sizes is elaborated in Case Study 3.

vi. Change the line length from 1km to 5km in step of 2km. Repeat step (i) to (v). This short circuit simulation study comprising of 3 fault locations, 3 fault resistances, 3 load sizes, and 3 line lengths is elaborated in Case Study 4. Through the short circuit simulation from step (i) to (vi), there will be a total 81 tests conducted in this research project comprising of 3 fault locations, 3 fault resistances, 3 load sizes, and 3 line lengths.

vii. Repeat steps (i) to (vi) for the relay pairs of R2-R1. In this case, the fault is simulated at line L2 instead of line L3. Relay R2 is the main relay whereas relay R1 is the backup relay. Given that grading margin for two relay pairs (R3-R2 and R2-R1) are to be identified for each case, the 81 cases are multiplied by two to become 162 cases.

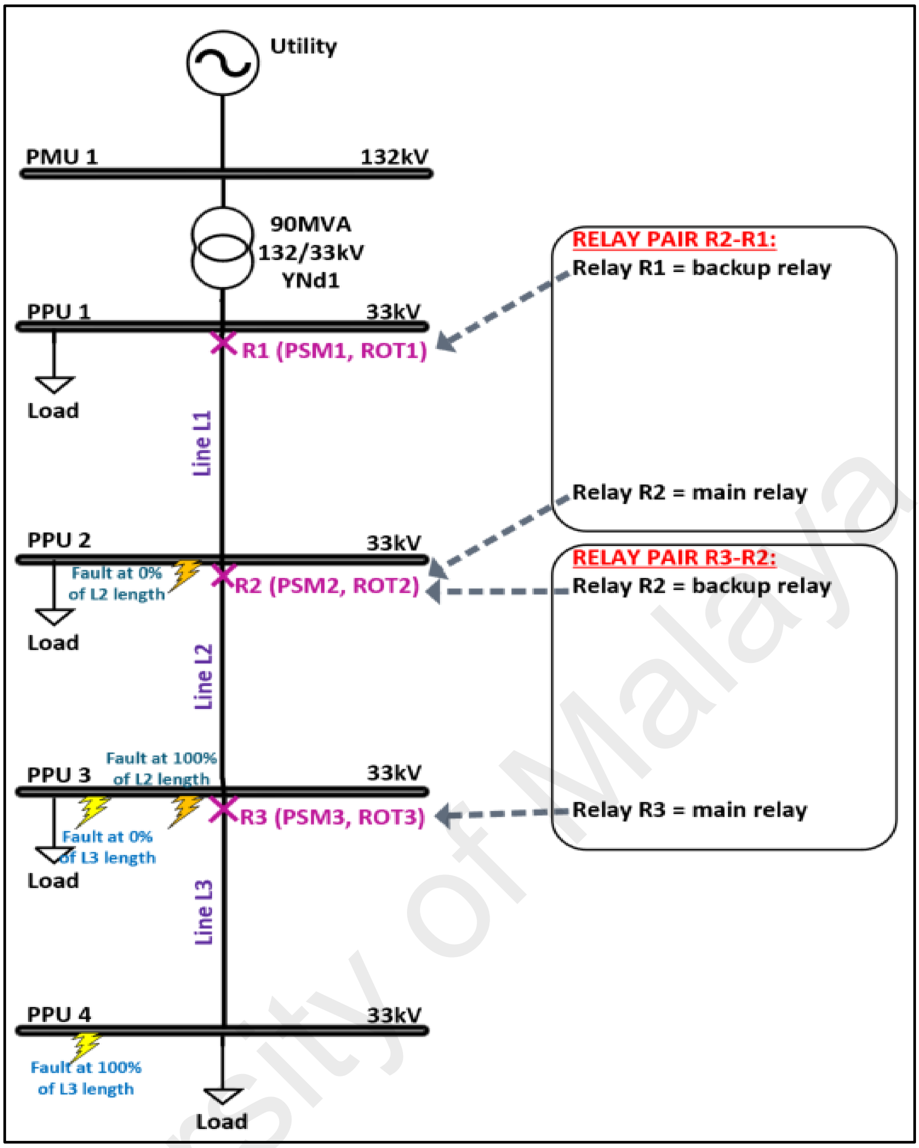

Figure 3.10: Network configuration for short circuit simulation for relay pairs R3-R2 and R2-R1.

3.7 Identification of the GM for the Main-Backup Relay Pairs

With the fault currents flowing through the relays recorded, the actual ROT for the main and backup relay can then be calculated to determine the relay grading margin for the main-backup relay pairs. Given that grading margin for two relay pairs (R3-R2 and R2-R1) are to be identified for each case, the 81 cases are multiplied by two to become 162 cases.

3.7.1 Hall's Method

The ROT for the main relay (R3) and backup relay (R2) can be calculated using the Equation 3.13 – Equation 3.15 as follows:

$$ROT_{R3} = TMS_3 \times \frac{0.14}{\left(\frac{I_{f_3}}{I_S}\right)^{0.02} - 1} \tag{3.13}$$

$$ROT_{R2} = TMS_2 \times \frac{0.14}{\left(\frac{I_{f_2}}{I_S}\right)^{0.02} - 1} \tag{3.14}$$

$$GM_{R3-R2_{(Hall's\ Method)}} = ROT_{R2} - ROT_{R3} \tag{3.15}$$

where I_{f_2} and I_{f_3} are the fault current flowing through relay R2 and relay R3 respectively during the simulation. ROT_{R2} and ROT_{R3} are the actual relay operating time for the recorded fault current. $GM_{R3-R2_{(Hall's\ Method)}}$ is the time interval between the operation of relay R2 and relay R3 for the recorded fault current when the relay pair is graded using Hall's Method.

3.7.2 Ravindranath's Method

The ROT for the main relay (R3) and backup relay (R2) can be calculated using the Equation as follows:

$$ROT_{R3} = TMS_3 \times \frac{0.14}{\left(\frac{I_{f_3}}{I_s}\right)^{0.02} - 1} \tag{3.16}$$

$$ROT_{R2} = TMS_2 \times \frac{0.14}{\left(\frac{I_{f_2}}{I_s}\right)^{0.02} - 1} \tag{3.17}$$

$$GM_{R3-R2_{(Ravindranath's\ Method)}} = ROT_{R2} - ROT_{R3} \tag{3.18}$$

where I_{f_2} and I_{f_3} are the fault current flowing through relay R2 and relay R3 respectively during the simulation. ROT_{R2} and ROT_{R3} are the actual relay operating time for the recorded fault current. $GM_{R3-R2(Ravindranath's\ Method)}$ is the time interval between the operation of relay R2 and relay R3 for the recorded fault current when the relay pair is graded using Ravindranath's Method.

3.8 Validation of the simulation results through real-time Hardware-in-the-Loop (HIL) experiment using OPAL-RT simulator

3.8.1 Hardware Setup

3.8.1.1 Overcurrent Relay

Figure 3.11: Mikro MK3000L overcurrent relay.

Figure 3.11 shows the numerical overcurrent relay used in the research project which is the Mikro MK3000L. To connect the MK3000L relay to OPAL-RT simulator, physical connections need to be established with reference to the typical relay wiring diagram in

Figure 3.12. The output contacts of the relay which are numbered 37 and 40 are connected to the positive terminal of the DC power supply. The output contacts of the relay which are numbered 38 and 41 are connected with separate resistors of value up to 1k**Ω**. The other nodes of the resistors are connected to the negative terminal of the DC power supply. The relay output contacts are in ‘Normally Open’ (NO) position. When the current at some particular phase exceeds the threshold value, the relay contacts of that particular phase will change to ‘Close’ position. The voltage will appear across the respectively connected resistor and therefore, sensed by the OPAL-RT simulator. As such, the tripping signal of the relay is sent back to the OPAL-RT simulator.

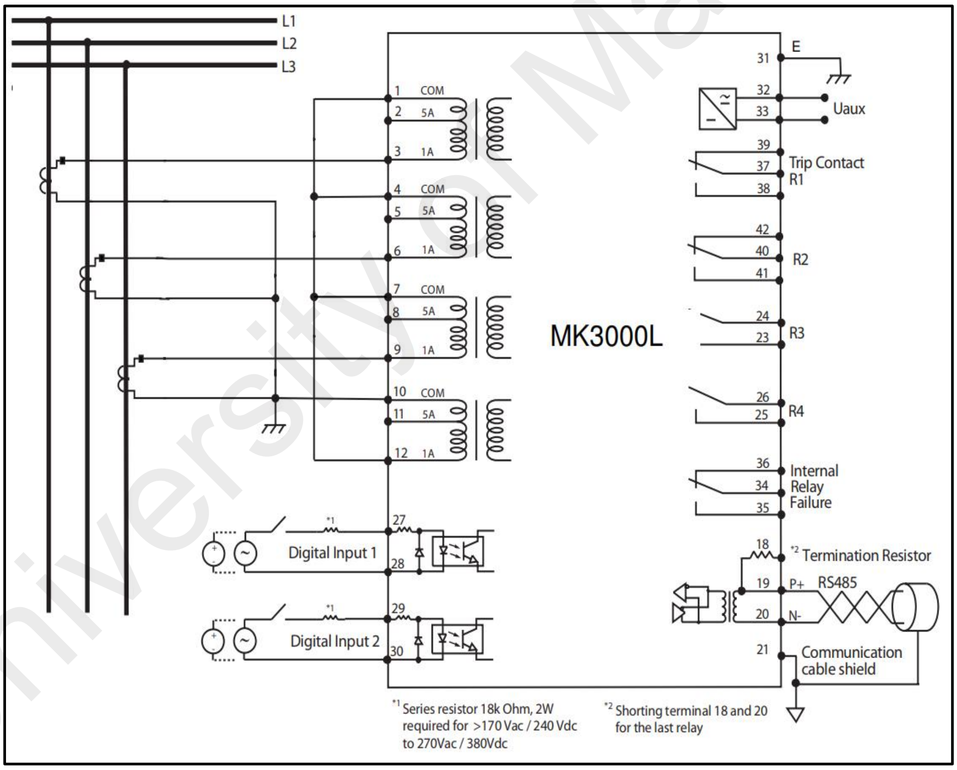

Figure 3.12: Typical Mikro MK3000L relay wiring connection diagram.

3.8.1.2 Real-time simulator

Figure 3.13 shows the real-time simulator that is used in this project which is the OPAL-RT OP5600. This rack-mounted simulator contains two compartments. The first compartment contains the analog and digital input/output (I/O) signal modules whereas the second compartment contains powerful processors. These processors ensure the accuracy of the generated signals in real-time simulations.

Figure 3.13: OPAL-RT OP5600 Simulator.

To ensure that the simulation can be conducted in real-time, the simulation time step needs to be small enough. The real-time simulator enables a time step of below of 10 microseconds which fulfills this condition. At the calculation speed of this range, a personal computer (PC) cannot update graphs and other monitoring channels in real time with all the data from the real-time digital simulator. Therefore, a useful feature of the real-time digital simulator is the RT-LAB software installed on a PC. It is the only tool for communication between the user and the simulator. The connection between the PC and the OPAL-RT is direct. Acquiring and monitoring the output signals in a time domain is possible via ScopeView tool in RT-LAB software.

Before the Simulink model can be compiled and executed in real-time on the Opal-RT real-time simulator, the model must be made compatible with RT-Lab software. The Simulink model used with RT-LAB must only display subsystems. The subsystem is a set of blocks that are placed inside one single block. In the RT-LAB platform, a subsystem is essential for distinguishing between computation elements and graphical user interface

(GUI) elements. Figure 3.14 displays two subsystems have been created for this research project in RT-LAB. The 33kV network model is placed in the subsystem labelled SM_grid, while the monitoring channels are placed in another subsystem labelled SC_scope.

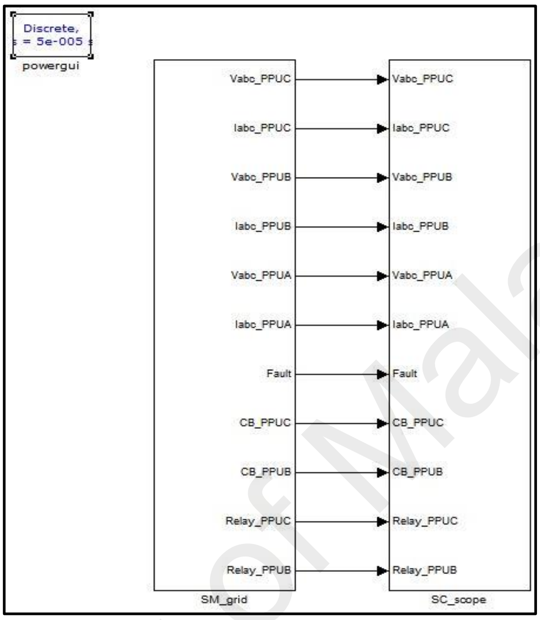

Figure 3.14: SM_grid and SC_scope subsystems in RT-LAB software.

Once the model is grouped into SM_grid and SC_scope subsystems, dedicated blocks called OpComm blocks are inserted into the subsystems. OpComm intercepts all incoming signals before sending the signals to computation blocks within a given subsystem. Inside the SC_scope subsystem block, there is one OpComm block inserted to allow for the selection of desired data acquisition ground to be used to acquire data from the model and to specify acquisition parameters. In the Figure 3.15 shown, some of the acquisition parameters include phase-to-phase voltages at PPU 1, PPU 2, and PPU 3, phase-to-phase currents at PPU 1, PPU 2, and PPU 3, signal of the relay at PPU 2 and PPU 3, and a signal of the circuit breaker at PPU 2 and PPU 3.

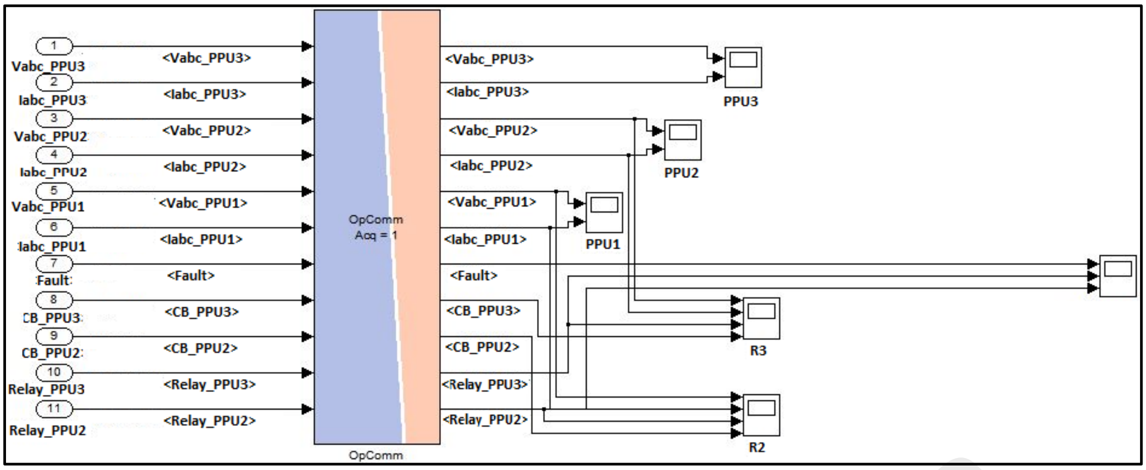

Figure 3.15: OpComm block in SC_scope subsystem.

RT-LAB comprises a library of blocks that can be included to provide access to the I/O cards. Each of the blocks refers to a function provided by the I/O board of the OPAL-RT simulator. Figure 3.16 shows the Digital Input block in RT-LAB while Figure 3.17 shows the Analog Output block in RT-LAB. Referring to the Figure 3.16 and Figure 3.17, parameters have been set to indicate to RT-LAB the location of Module A corresponding to the respective Digital Input and Analog Output blocks. The test system modelled in RT-LAB is illustrated in Figure 3.18.

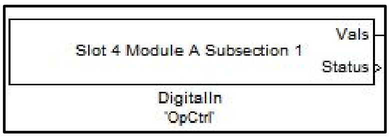

Figure 3.16: Digital Input block in RT-LAB.

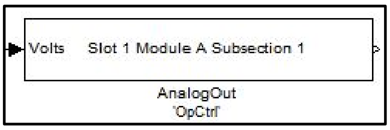

Figure 3.17: Analog Output block in RT-LAB software.

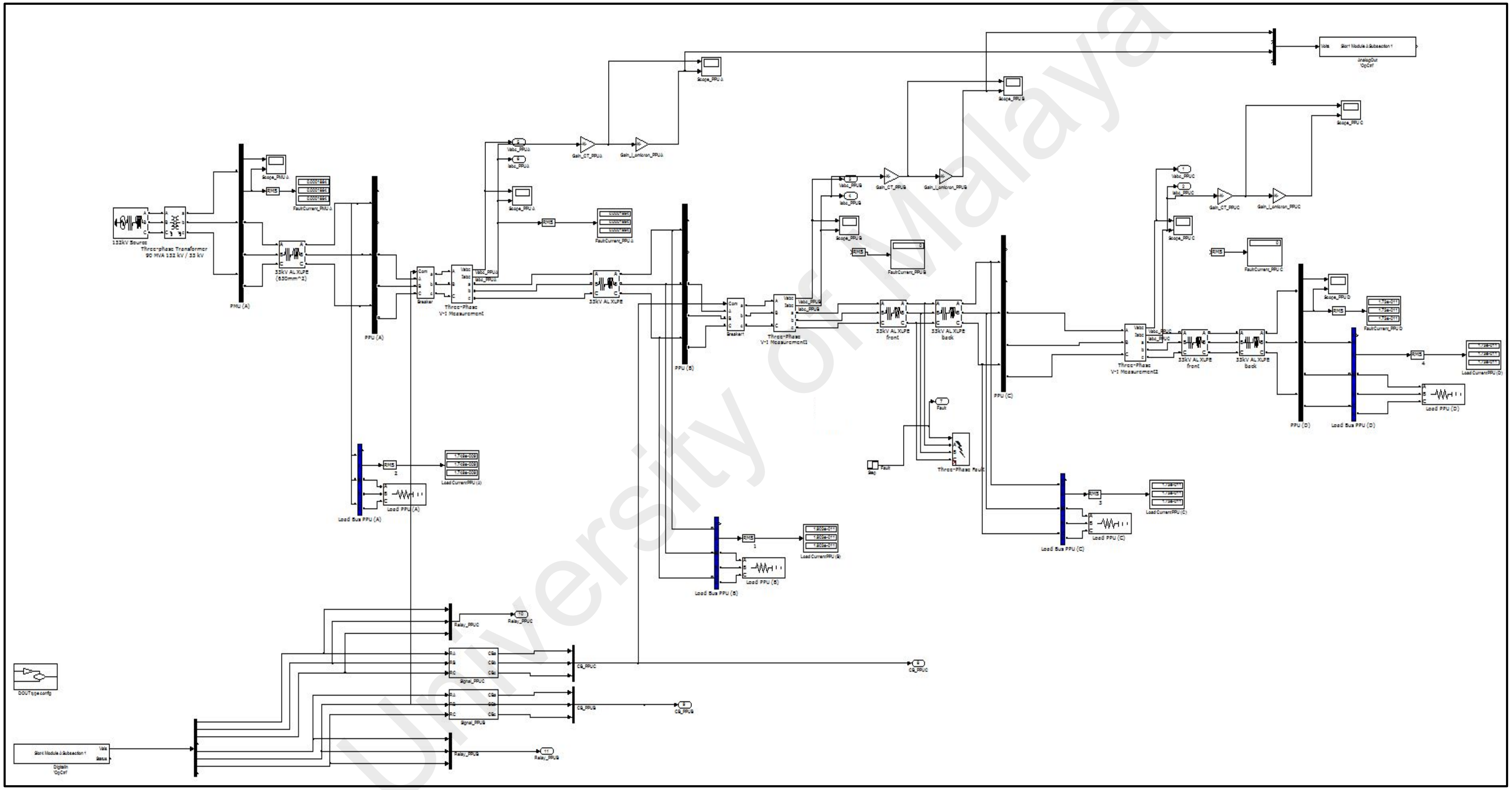

Figure 3.18: Modelling of the test system in RT-LAB software.

3.8.1.3 Current amplifier

Actual protection relays are connected to the low voltage side of the current transformer. However, the current transformer is only modelled in the OPAL-RT simulator environment. The current amplifier needs to be used to export current signals from the real-time digital simulator to the relay. The current amplifier receives the control signals (voltage) from the real-time simulator, amplify them to the current signal of desired values, and then sends those currents to the relay. OMICRON CMA 156 amplifier is used for this purpose. Figure 3.19 shows the CMA 156 current amplifier that is used in this research project.

Figure 3.19: CMA 156 Current Amplifier.

3.8.2 Overall Hardware Configuration

Figure 3.20 depicts the block diagram of the overall hardware configuration for HIL experiment using Opal-RT real-time simulator to validate the simulated results from Simulink. The Simulink model is first compiled and loaded into the Opal-RT real-time simulator using the RT-LAB software. Once the fault is simulated at a specific time, the fault current from the analog outputs of the OPAL-RT simulator is amplified using the OMICRON CMA 156 current amplifier and fed into the CT input terminal of the Mikro MK3000L relay. The relay contacts will close upon sensing the fault current. The digital output of the relay is connected to the digital input of the real-time simulator. When the relay trips, the digital input of the real-time simulator will detect the trip signal and opens the circuit breaker in the simulator environment. The fault can then be isolated. Real-time simulation test results can be accessed from the console generated by the RT-LAB software.

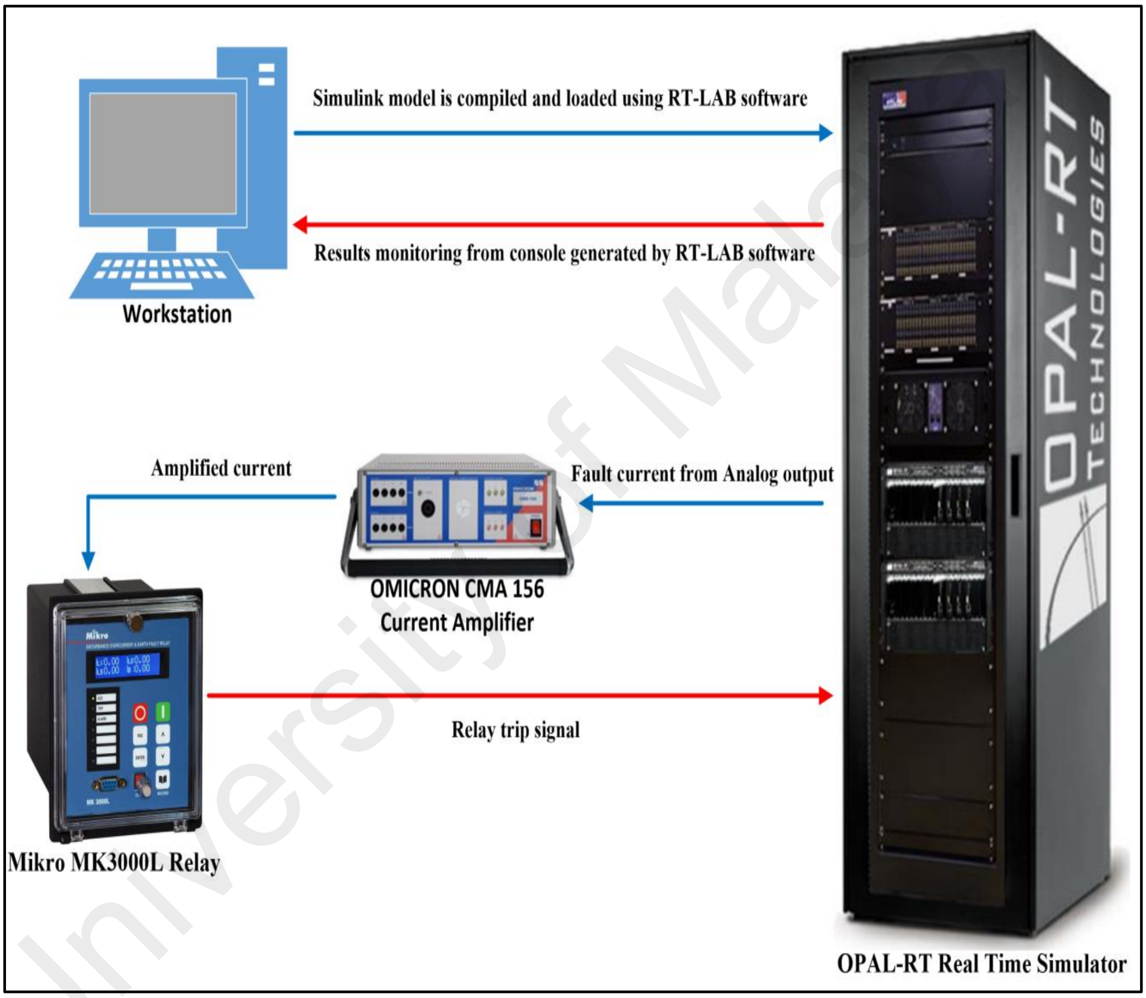

Figure 3.20: Block diagram of relay testing using Opal-RT real-time simulator.

CHAPTER 4: RESULTS AND DISCUSSION

4.1 Introduction

This chapter presents the results from short circuit analysis, relay grading using the two different methods, short circuit simulation in Simulink, and validation of simulation results through HIL experiment using the real-time simulator. The time-overcurrent curves for the relay pairs R3-R2 and R2-R1 are also plotted for both the grading methods for better visualization. The relay tolerance curve is also shown in this chapter.

4.2 Results of Short Circuit Analysis in the Radial Distribution Network

The Simulink model for the 33kV radial distribution network has been developed in Section 3.3. In this model, there is a total of four 33kV PPUs, which are PPU 1, PPU 2, PPU 3, and PPU 4.

In this short circuit study of the selected test case, a three-phase bolted fault is first simulated at respective PPU (PPU 1, PPU 2, PPU 3, and PPU 4) in the radial distribution network. The total RMS fault current measured at the location where the fault is applied is tabulated in Table 4.1.

Table 4.1: Maximum fault current measured at each PPU where the fault is applied.

Fault Location	Maximum Fault Current, $I_{sc_{max}}$(A)
PPU 1	18510
PPU 2	11230
PPU 3	7687
PPU 4	5711

The left column of Table 4.1 represents the location of the faulted PPU while the right column of Table 4.1 represents the total fault current measured at the faulted bus. Busbar of PPU 1 is located nearest to the source, whereas busbar of PPU 4 is located furthest from source.

As shown in Table 4.1, it can be observed that the maximum fault current decreases when fault location is varied from busbar of PPU 1 to busbar of PPU 4. As the current flow further away from the source to PPU 4, the total current decreases due to the increase in impedance of the distribution cable.

4.3 Results of Overcurrent Relay Grading

The relay grading procedures are presented in Table 4.2. As discussed in Sub-Section 3.3.5, the chosen CT primary current chosen must be higher than the maximum load current determined through the load flow analysis, whereas the CT secondary current is 1A. Hence, for this case study, the CT ratio selected shall be 1500:1. The total load current is 1331.5A. PSM of 1.0 is considered based on Step 2 of Table 4.2. The calculated setting current $I_S$is 1500A. The CT ratio and PSM values are assumed to be the same for all the relays in this network. The values of the total load current, CT ratios, and maximum fault current at respective PPUs are presented in Table 4.3.

Table 4.2: Calculation for PSM and I_s

Step 1: To calculate the minimum setting current, $I_{s_{min}}$	The setting current safety margin is 1.05. $I_{s_{\min}} = Total\ Load\ Current \times Setting\ Current\ Safety\ Margin$ $I_{s_{\min}} = 1331.5A \times 1.05$ $I_{s_{\min}} = 1398.075A$
Step 2: To calculate the plug setting multiplier (PSM)	$PSM = \frac{I_{s_{\min}}}{CT\ ratio}$ $PSM = \frac{1398.075A}{1500A} = 0.9325$ Hence, the next higher PSM of 1.0 is selected.
Step 3: To calculate the setting current, I_s	$I_s = PSM \times CT\ ratio$ $I_s = 1 \times 1500A$ $I_s = 1500A$

Table 4.3: PSM and CT ratio for relays.

Fault Location	Relay	CT ratio	PSM	Maximum Fault Current, $I_{sc_{max}}$(A)
PPU 1	R1	1500/1	1.0	18510
PPU 2	R2	1500/1	1.0	11230
PPU 3	R3	1500/1	1.0	7687
PPU 4	-	-	-	5711
Total Load Current = 1331.5A				

4.3.1 Results of Relay Grading using Hall's Method

Using the data from Table 4.2 and Table 4.3, the overcurrent relays are graded using Hall's Method. The time multiplier setting (TMS) for the respective overcurrent relay R3, R2, and R1 are calculated based on steps listed in Table 4.4. The grading will be done in pairwise which is R3-R2 and R2-R1. The calculated TMS for respective relay R1, R2, and R3 are tabulated in Table 4.5.

Table 4.4: Calculation for TMS for relay R3, R2, and R1 – using Hall's Method

Main-Backup Relay Pair	TMS Calculation
R3-R2	$TMS_3 = 0.01$ $ROT_3 = TMS_3 \times \frac{0.14}{\left(\frac{I_{sc_{\max 4}}}{I_s}\right)^{0.02} - 1}$ $ROT_3 = 0.01 \times \frac{0.14}{\left(\frac{5711}{1500}\right)^{0.02} - 1} = 0.0517s$ $ROT_2 = 0.0517 + 0.3 = 0.3517s$ $TMS_2 = ROT_2 \times \frac{\left(\frac{I_{sc_{\max 4}}}{I_s}\right)^{0.02} - 1}{0.14}$ $TMS_2 = 0.3517 \times \frac{\left(\frac{5711}{1500}\right)^{0.02} - 1}{0.14} = 0.07$
R2-R1	$TMS_2 = 0.07$ $ROT_2 = TMS_2 \times \frac{0.14}{\left(\frac{I_{sc_{\max 3}}}{I_s}\right)^{0.02} - 1}$ $ROT_2 = 0.07 \times \frac{0.14}{\left(\frac{7687}{1500}\right)^{0.02} - 1} = 0.2950s$ $ROT_1 = 0.2950 + 0.3 = 0.5950s$ $TMS_1 = ROT_1 \times \frac{\left(\frac{I_{sc_{\max 3}}}{I_s}\right)^{0.02} - 1}{0.14}$ $TMS_1 = 0.5950 \times \frac{\left(\frac{7687}{1500}\right)^{0.02} - 1}{0.14} = 0.14$

Table 4.5: TMS for respective relay upon relay grading using Hall's Method

Relay	TMS
R3	0.01
R2	0.07
R1	0.14

4.3.2 Results of Relay Grading using Ravindranath's Method – Proposed by (Ravindranath & Chander, 1977)

Using the data from Table 4.3 and Table 4.4, the overcurrent relays are graded using Ravindranath's Method as proposed by (Ravindranath & Chander, 1977). The time multiplier setting (TMS) for the respective overcurrent relay R3, R2, and R1 are calculated based on steps listed in Table 4.6. The calculated TMS for respective relay R1, R2, and R3 are tabulated in Table 4.7.

Table 4.6: Calculation for TMS for relay R3, R2, and R1 – using Ravindranath's Method.

Main-Backup Relay Pair	TMS Calculation
R3-R2	$TMS_3 = 0.01$ $ROT_3 = TMS_3 \times \frac{0.14}{\left(\frac{I_{sc_{\max 3}}}{I_s}\right)^{0.02} - 1}$ $ROT_3 = 0.01 \times \frac{0.14}{\left(\frac{7687}{1500}\right)^{0.02} - 1} = 0.0421s$ $ROT_2 = 0.0421 + 0.3 = 0.3421s$ $TMS_2 = ROT_2 \times \frac{\left(\frac{I_{sc_{\max 3}}}{I_s}\right)^{0.02} - 1}{0.14}$ $TMS_2 = 0.3421 \times \frac{\left(\frac{7687}{1500}\right)^{0.02} - 1}{0.14} = 0.09$
R2-R1	$TMS_2 = 0.09$ $ROT_2 = TMS_2 \times \frac{0.14}{\left(\frac{I_{sc_{\max 2}}}{I_s}\right)^{0.02} - 1}$ $ROT_2 = 0.09 \times \frac{0.14}{\left(\frac{11230}{1500}\right)^{0.02} - 1} = 0.3067s$ $ROT_1 = 0.3067 + 0.3 = 0.6067s$ $TMS_1 = ROT_1 \times \frac{\left(\frac{I_{sc_{\max 2}}}{I_s}\right)^{0.02} - 1}{0.14}$ $TMS_1 = 0.6067 \times \frac{\left(\frac{11230}{1500}\right)^{0.02} - 1}{0.14} = 0.18$

Table 4.7: TMS for respective relay R3, relay R2, and relay R1 upon relay grading using Ravindranath's Method

Relay	TMS
R3	0.01
R2	0.09
R1	0.18

The time multiplier setting (TMS) for relay R3 graded using Ravindranath's Method is similar to the TMS for relay R3 graded using Hall's Method that is 0.01. TMS for both the relay R2 and R3 graded using Ravindranath's Method is higher in comparison to when the relay R2 and R3 graded using Hall's Method.

4.4 Perform Short Circuit Current Simulation and Record Short Circuit Current under Various Power System Dynamic Scenarios

Upon obtaining the TMS and PSM for relay setting, the model is simulated under the various power system scenario following the steps for short circuit simulation discussed in Section 3.6. Out of the 162 test cases comprising of different power system scenarios for short circuit simulation, Test no. 73 has been selected for the explanation in Section 4.5. Table 4.8 shows the parameters of the power system scenario in Test no. 73.

Table 4.8: Parameter values for Test no. 73.

Parameters	Value
Cable length	5km
Fault resistance	0Ω
Fault location	0%
Load size	100%

The fault current seen by the relay pair R2 and R1 are tabulated in Table 4.9:

Table 4.9: Fault current seen by relay R2 and relay R1.

Relay	Fault Current saw by Relay, I_f (A)
R2	11230
R1	11470

4.5 Identification of the GM for the Main-Backup Relay Pairs

With the fault currents flowing through the relays recorded, the actual ROT for the main and backup relay can then be calculated to determine the relay grading margin for the main-backup relay pairs. For Section 4.5.1 and Section 4.5.2, the relay pair R2-R1 is considered. The same calculation steps are applicable for relay pair R3-R2.

4.5.1 Hall's Method

The ROT for the main relay (R2) and backup relay (R1) can be calculated using the steps shown in Table 4.10. The time overcurrent curve for the R2-R1 relay pairs is shown in Figure 4.1. As seen in the graphical representation, when the I_f seen by the relay R2 and R1 is 11230A, the difference of the relay operating time of both relays would be 0.24s. This grading margin of the R2-R1 relay pair which is less than 0.3s indicates that the grading margin is jeopardized. When a fault occurs, both main relay R2 and backup relay R1 will operate. As a result, more customers are affected where customers connected to PPU 2 will also experience disruptions in electricity supply due to the operation of relay R1.

Table 4.10: Calculation for Grading Margin (GM) for R2-R1 relay pair – using Hall's Method

Main-Backup Relay Pair	Grading Margin (GM) Calculation
R2-R1	$TMS_2 = 0.07$ $ROT_{R2} = TMS_2 \times \frac{0.14}{\left(\frac{I_{f_2}}{I_s}\right)^{0.02} - 1}$ $ROT_{R2} = 0.07 \times \frac{0.14}{\left(\frac{11230}{1500}\right)^{0.02} - 1} = 0.24s$ $TMS_1 = 0.14$ $ROT_{R1} = TMS_1 \times \frac{0.14}{\left(\frac{I_{f_1}}{I_s}\right)^{0.02} - 1}$ $ROT_{R1} = 0.14 \times \frac{0.14}{\left(\frac{11470}{1500}\right)^{0.02} - 1} = 0.47s$ $GM_{R2-R1_{(Hall's\ Method)}} = ROT_{R1} - ROT_{R2} = 0.23s$

Simulations were repeated for a total of 162 tests following the steps in Section 3.6. The calculated relay grading margin for R3-R2 and R2-R1 relay pairs as a result from the repetitive simulations under various power system dynamic scenarios as discussed in Section 3.6 are tabulated in Appendix A.

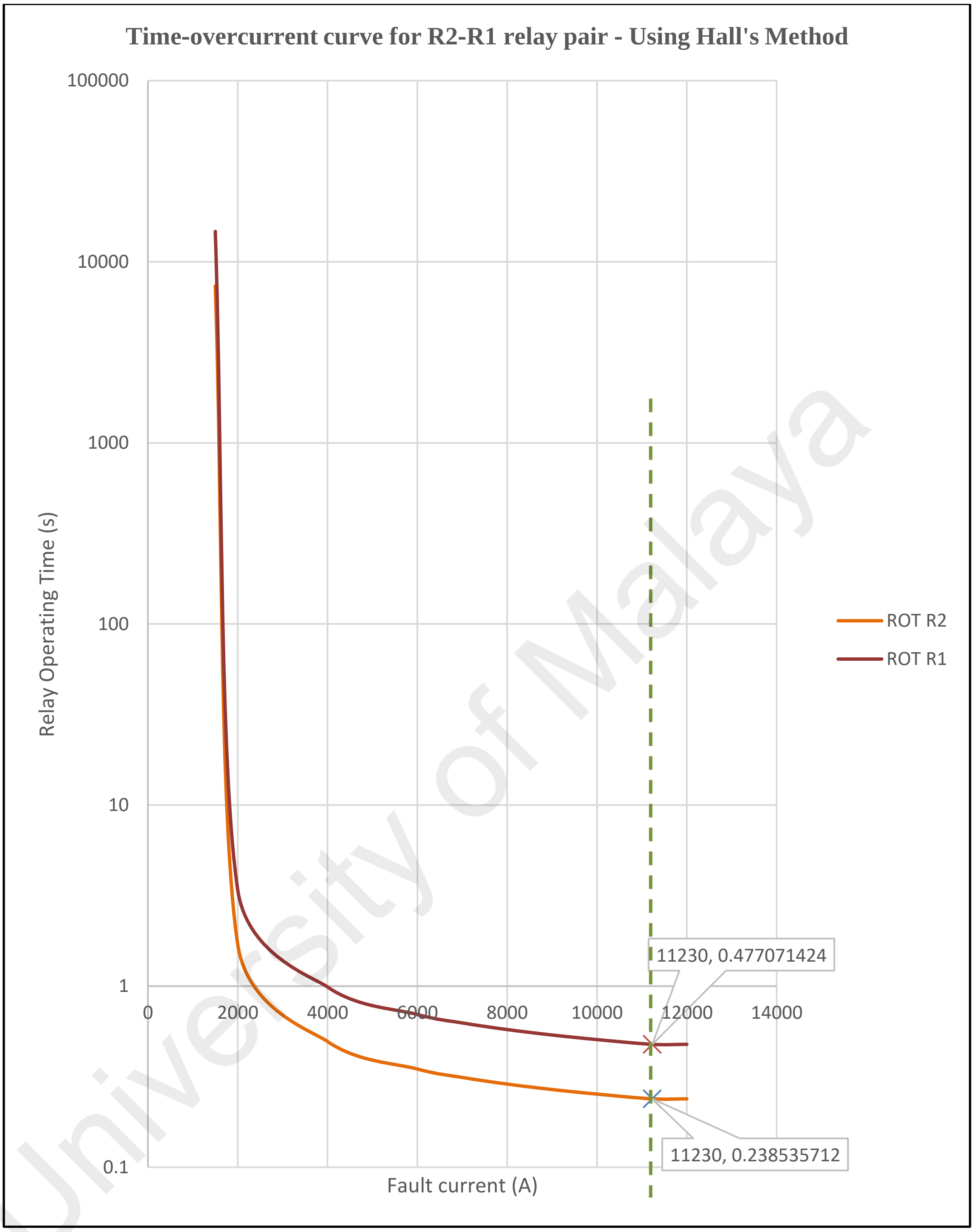

Figure 4.1: Time-overcurrent curve for R2-R1 relay pair – using Hall's Method.

4.5.2 Ravindranath's Method

The ROT for the main relay (R2) and backup relay (R1) can be calculated and shown in Table 4.11 below:

Table 4.11: Calculation for Grading Margin (GM) for R2-R1 relay pair – using Ravindranath's Method

Main-Backup Relay Pair	Grading Margin (GM) Calculation
R2-R1	$TMS_2 = 0.09$ $ROT_{R2} = TMS_2 \times \frac{0.14}{\left(\frac{I_{f_2}}{I_s}\right)^{0.02} - 1}$ $ROT_{R2} = 0.09 \times \frac{0.14}{\left(\frac{11230}{1500}\right)^{0.02} - 1} = 0.31s$ $TMS_1 = 0.18$ $ROT_{R1} = TMS_1 \times \frac{0.14}{\left(\frac{I_{f_1}}{I_s}\right)^{0.02} - 1}$ $ROT_{R1} = 0.18 \times \frac{0.14}{\left(\frac{11470}{1500}\right)^{0.02} - 1} = 0.61s$ $GM_{R2-R1_{(\text{Ravindranath's } Method)}} = ROT_{R1} - ROT_{R2}$ $GM_{R2-R1_{(\text{Ravindranath's } Method)}} = 0.30s$

Time overcurrent curve for the R2-R1 relay pair is shown in Figure 4.2. As seen in the graphical representation, when the I_f seen by the relay R2 and R1 is 11230A, the difference of the relay operating time of both relays would be 0.31s.

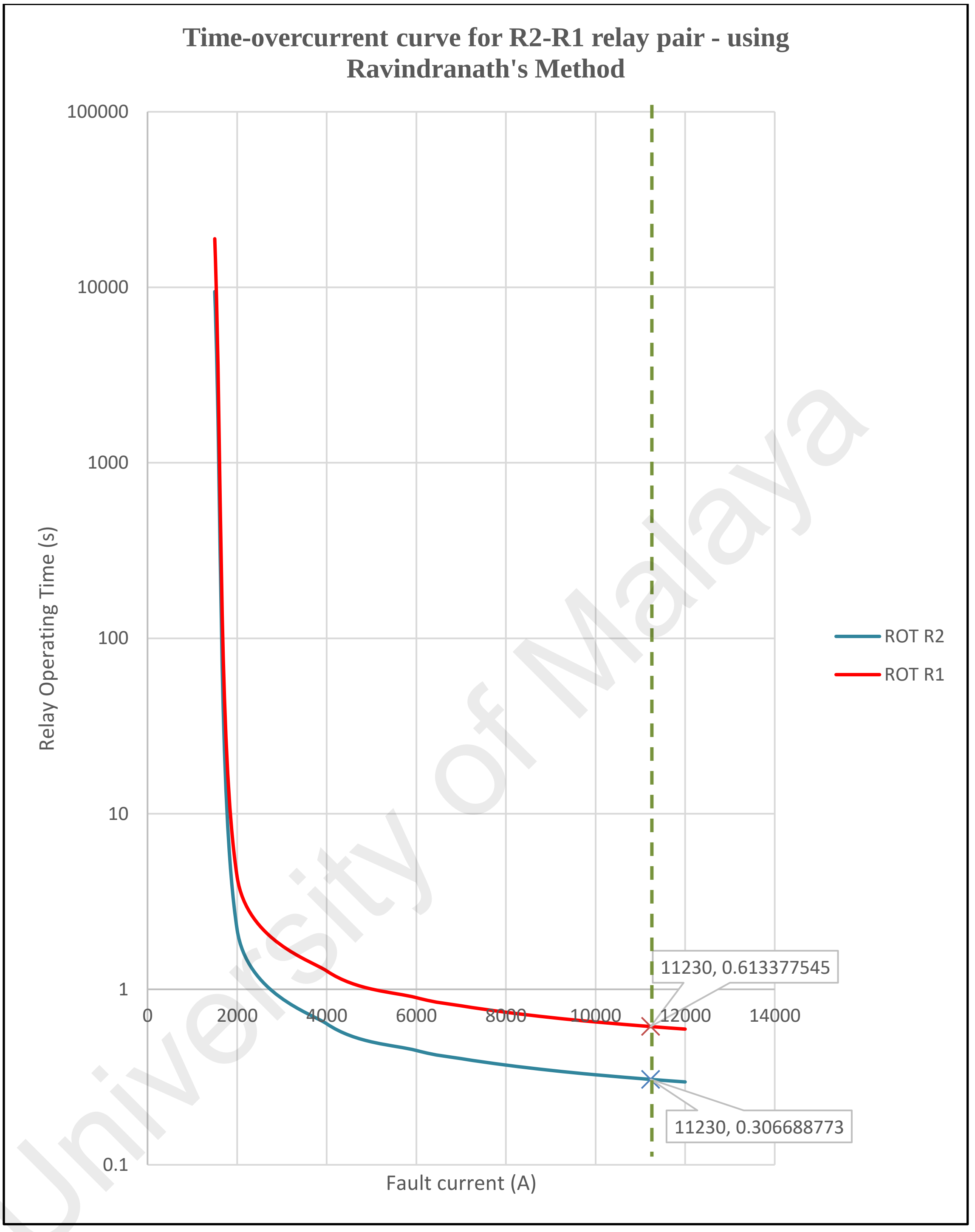

Figure 4.2: Time-overcurrent curve for R2-R1 relay pair – using Ravindranath's Method.

Simulations were repeated for a total of 162 tests following the steps in Section 3.6. The calculated relay operating time for the R3-R2 and R2-R1 relay pair as a result from the repetitive simulations under various power system dynamic scenarios as discussed in Section 3.6 are tabulated in Appendix A.

4.5.3 Discussion on Sensitivity Analysis in Short Circuit Current Simulation

Section 4.5.1 and Section 4.5.2 shows an example to calculate the actual ROT for the main and backup relay and determine the relay grading margin for the relay pair R2-R1 using the recorded fault currents flowing through the relays in Test no. 73. The same calculation steps are applicable for relay pair R3-R2. Through the short circuit simulation from step (i) to (v) in Section 3.6, there will be a total 81 tests conducted in this research project comprising of 3 fault locations, 3 fault resistances, 3 load sizes, and 3 line lengths. Given that grading margin for two relay pairs (R3-R2 and R2-R1) are to be identified for each case, the 81 cases are multiplied by two to become 162 cases. By applying the same calculation steps shown Section 4.5.1 and Section 4.5.2, the grading margin for the relay pairs R3-R2 and R2-R1 for all the 162 cases would have been determined.

In the short circuit current simulation, sensitivity analysis is adopted to investigate the effects of the power system dynamics (fault location, fault resistance, load size, and cable length) on the grading margin of the relay pairs R3-R2 and R2-R1. In Section 3.6, four case studies have been developed to investigate the effects of the power system dynamics (fault location, fault resistance, load size, and cable length) on the grading margin of the relay pairs. In this Section 4.5.3, the results of the 4 case studies is presented. The grading margin for relay pairs determined using the calculation steps shown in the Section 4.5.1 and Section 4.5.2 will be plotted against the varying parameters of respective power system dynamics (fault location, fault resistance, load size, and cable length) to investigate the effects of the power system dynamics (fault location, fault resistance, load size, and cable length) on the grading margin of the relay pairs R3-R2 and R2-R1.

a. Results of Case Study 1

Case Study 1 aims to investigate the effect of fault location on the grading margin for the relay pairs. Case Study 1 comprises of varying 3 fault locations which is d_F = 0%, d_F

= 50%, and d_F = 100%. Figure 4.3 presents the effect of varying fault location on the grading margin of the relay pairs with fault resistance, $R_F = 0\Omega$, load size = 0%, and cable length, l = 1km. This means that the outcome from the Figure 4.3 is purely investigating the effect of the fault resistance on the grading margin for the relay pairs, which is free from influence of fault resistance, load size, and cable length.

Based on Figure 4.3, the grading margin increases with the increase of fault location. The grading margin for the main-backup relay pairs of R3-R2 and R2-R1 using Ravindranath's Method increases from 0.31s with the fault location increasing from 0% to 100%. For the case in which Hall's Method is used to grade the relays, the grading margin for the main-backup relay pairs of R3-R2 and R2-R1 using Hall's Method also increases with the fault location increasing from 0% to 100%. For relay pairs of R3-R2 graded using Hall's Method, the grading margin of the relay pairs increase from 0.29s to 0.30s when fault location increases from 0% to 100%. For relay pairs of R2-R1 graded using Hall's Method, the grading margin of the relay pairs increase from 0.28s to 0.31s when fault location increases from 0% to 100%.

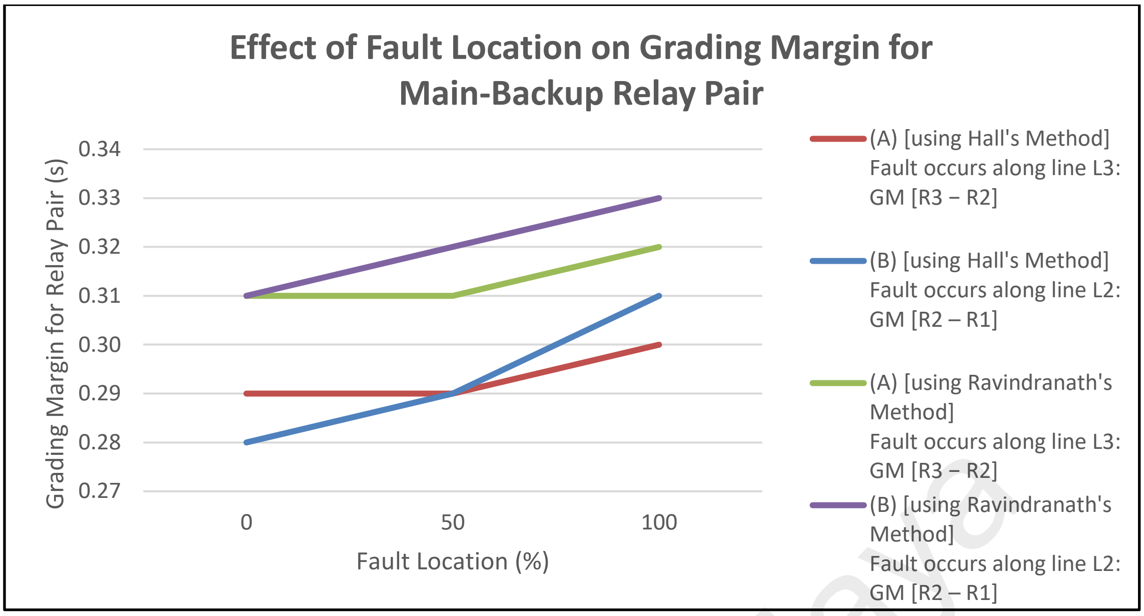

Figure 4. 3: Effect of varying fault location, d_F on grading margin for main-backup relay pair with fault resistance, $R_F = 0\Omega$, load size = 0%, and cable length, l = 1km.

b. Results of Case Study 2

Case Study 2 aims to investigate the effect of fault resistance on the grading margin for the relay pairs. Case Study 2 comprises of varying 3 fault resistances (R_F = 0 Ω, R_F = 5 Ω, and R_F = 10 Ω) and 3 fault locations (d_F = 0%, d_F = 50%, and d_F = 100%). Figure 4.4 presents the effect of varying fault resistance on grading margin for main-backup relay pair with fault location, $d_F = 0\%$, load size = 0%, and cable length, l = 1km. This means that the outcome from the Figure 4.4 is purely investigating the effect of the fault resistance on the grading margin for the relay pairs, which is free from influence of fault location, load size, and cable length.

Based on Figure 4.4, the grading margin increases with the increase of fault resistance. The grading margin for the main-backup relay pairs of R3-R2 and R2-R1 using Ravindranath's Method begin to increase from 0.31s for fault resistance increasing from 0 Ω to 10 Ω. For the case in which Hall's Method is used to grade the relays, the grading margin for the main-backup relay pairs of R3-R2 and R2-R1 also increases with the fault resistance increasing from 0 Ω to 10 Ω.

Nonetheless, since Case Study 2 also comprises of the varying fault locations, the effect of the fault location on the grading margin for relay pairs in Case Study 1 as discussed in Section 4.5.3(a) is still valid. In Case Study 1, the grading margin increases with fault location increasing from d_F = 0% to d_F = 100%, in steps of 50%.

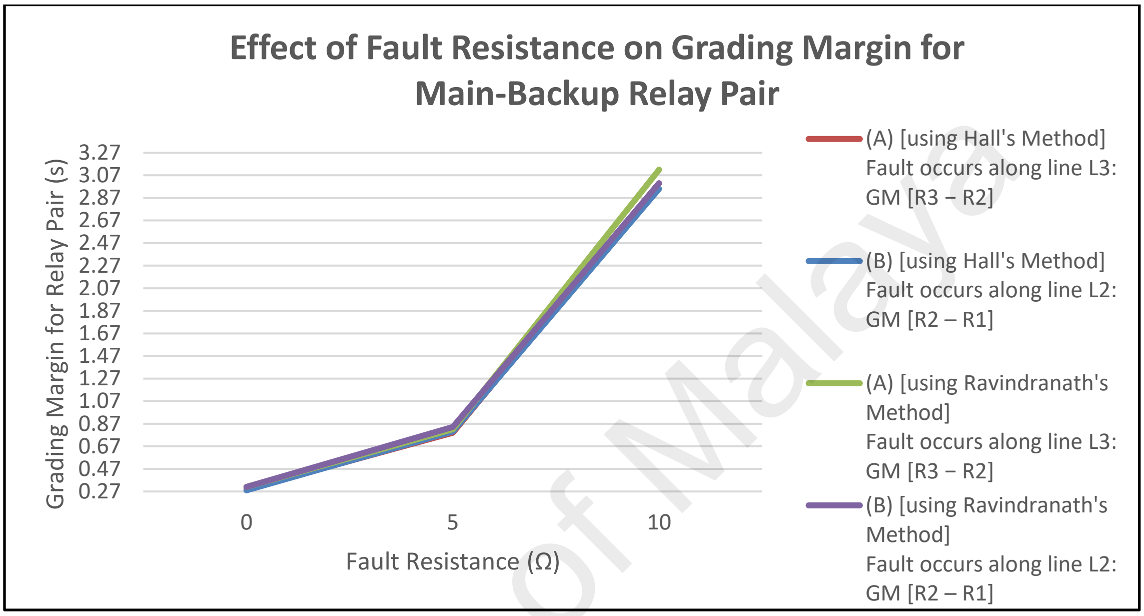

Figure 4. 4: Effect of varying fault resistance, R_F on grading margin for main-backup relay pair with fault location, $d_F =$ 0%, load size = 0%, and cable length, *l*=1km.

c. Results of Case Study 3

Case Study 3 aims to investigate the effect of load size on the grading margin for the relay pairs. Case Study 3 comprises of varying 3 load sizes (L = 0%, L = 50%, and L = 100%). 3 fault resistances (R_F = 0 Ω, R_F = 5 Ω, and R_F = 10 Ω), and 3 fault locations (d_F = 0%, d_F = 50%, and d_F = 100%). Figure 4.5 presents the effect of load size on grading margin for main-backup relay pair with fault location, $d_F =$ 0%, fault resistance, $R_F =$ 0Ω, and cable length, *l* = 1km. This means that the outcome from the Figure 4.5 is purely investigating the effect of the load size on the grading margin for the relay pairs which is free from influence of fault location, fault resistance and cable length.

Based on Figure 4.5, the grading margin is constant with the increase of load size. The grading margin for the main-backup relay pairs of R3-R2 and R2-R1 using Ravindranath's Method is constant at 0.31s. For the case in which Hall's Method is used to grade the main-backup relay pair, the grading margin for R3-R2 relay pair is constant at 0.29s while the grading margin for R2-R1 relay pair is constant at 0.28s. This is due to the reason that the current transformer is sized with the consideration of full load connected to the network. Therefore, the same current transformer ratio is used for the network whether 100% load is connected to the network or no load is connected to the network. With the same current transformer ratio used, PSM and the TMS for relays R1, R2, and R3 are the same irrespective to the load size connected to the network. As such, it is justified that grading margin for the main-backup relay pair is constant with the increase of load size.

Nonetheless, since Case Study 3 also comprises of the varying 3 fault locations and 3 fault resistances, the effect of the fault location on the grading margin for relay pairs in Case Study 1 discussed in Section 4.5.3(a) and Case Study 2 discussed in Section 4.5.3(b) is still valid in Case Study 3. In Case Study 1, the grading margin increases with fault location increasing from d_F = 0% to d_F = 100%, in steps of 50%. In Case Study 2, the grading margin increases with fault resistance increasing from R_F = 0Ω to R_F = 10Ω, in steps of 5Ω.

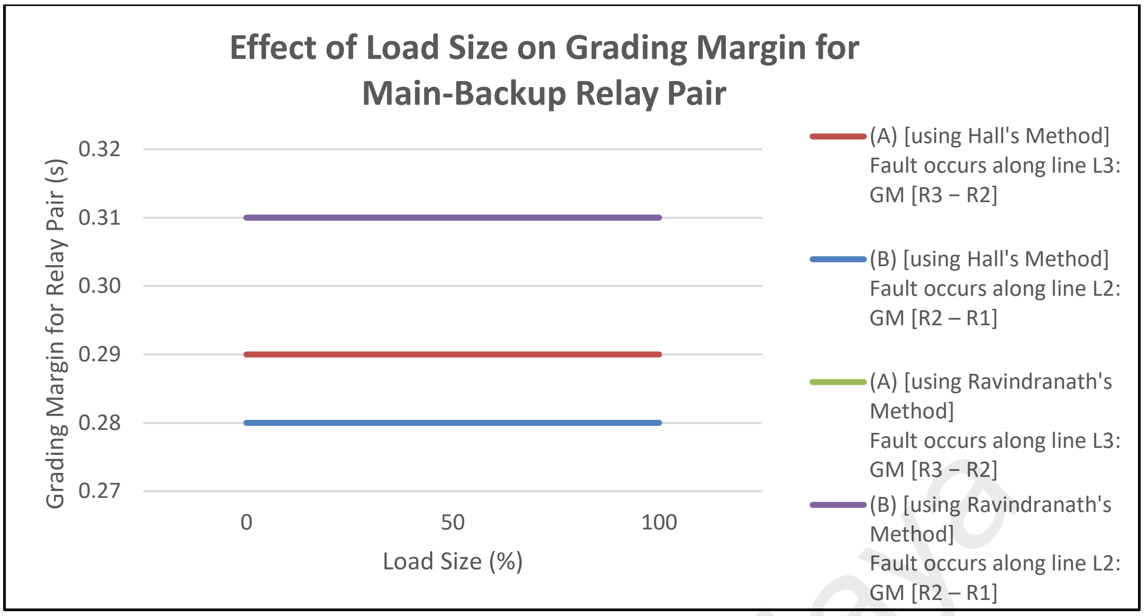

Figure 4. 5: Effect of varying load size, *L* on grading margin for main-backup relay pair, with fault location, $d_F = 0\%$, fault resistance, $R_F = 0\Omega$, and cable length, *l*=1km.

d. Results of Case Study 4

Case Study 4 aims to investigate the effect of cable length on the grading margin for the relay pairs. Case Study 4 comprises of varying 3 cable lengths (*l* = 1km, *l* = 3km, and *l* = 5km), 3 load sizes (*L* = 0%, *L* = 50%, and *L* = 100%), 3 fault resistances (R_F = 0 Ω, R_F = 5 Ω, and R_F = 10 Ω), and 3 fault locations (d_F = 0%, d_F = 50%, and d_F = 100%). Figure 4.6 presents the effect of cable length on grading margin for main-backup relay pair with fault location, $d_F = 0\%$, fault resistance, $R_F = 0\Omega$, and load size, *L* = 0%.

Based on Figure 4.6, the grading margin decreases with the increase of cable length. The grading margin for the main-backup relay pairs of R3-R2 and R2-R1 using Ravindranath's Method decrease from 0.31s to 0.30s with the cable length increasing from 1km to 5km. For the case in which Hall's Method is used to grade the relays, the grading margin for the main-backup relay pairs of R3-R2 and R2-R1 using Ravindranath's Method also decrease to 0.25s with the cable length increasing from 1km to 5km.

Nonetheless, since Case Study 4 also comprises of the varying 3 fault locations, 3 fault resistances and 3 load sizes, the effect of the respective power system dynamic (fault location, fault resistance, and load size) on the grading margin for relay pairs in Case Study 1 discussed in Section 4.5.3(a), Case Study 2 discussed in Section 4.5.3(b), and Case 3 discussed in Section 4.5.3(c) is still valid in Case Study 4. The explanation is similar to the discussion in Case Study 1, Case Study 2, and Case Study 3. In Case Study 1, the grading margin increases with fault location increasing from d_F = 0% to d_F = 100%, in steps of 50%. In Case Study 2, the grading margin increases with fault resistance increasing from R_F = 0Ω to R_F = 10Ω, in steps of 5Ω. In Case Study 3, the grading margin maintains with no change with load size increasing from L = 0% to L = 100%, in steps of 50%.

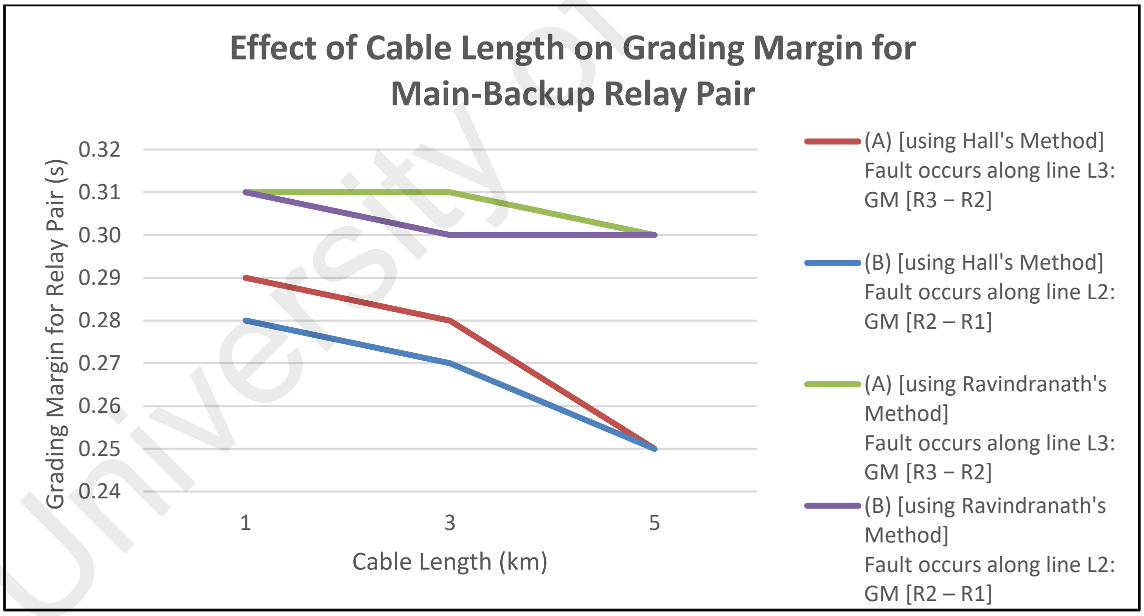

Figure 4. 6: Effect of cable length, l on grading margin for main-backup relay pair with fault location, $d_F = 0\%$, fault resistance, $R_F = 0\Omega$, and load size, L=0%.

4.5.4 Summary of Section 4.5

Upon the completion of sensitivity analysis to investigate the effects of the power system dynamics (fault location, fault resistance, load size, and cable length) on the grading margin of the relay pairs, the grading margin results for the relay pairs of R3-R2 and R2-R1 from Appendix A are presented in graphical form in Section 4.5.4.1 (for relays graded using Hall's Method) and Section 4.5.4.2 (for relays graded using Ravindranath's Method). Any grading margin below 0.3s indicates that the grading margin is jeopardized. When a fault occurs, relay closest to the fault location should operate and clear the fault. Referring to Figure 3.10, for the relay pair of R2-R1, only the main relay R2 should operate for a fault occurring at line L2. So, only customers connected to PPU 3 and PPU4 will experience disruptions in electricity supply. However, if the grading margin is jeopardized, both main relay R2 and backup relay R1 will operate. As a result, more customers are affected where customers connected to PPU 2 will also experience disruptions in electricity supply due to the operation of relay R1.

4.5.4.1 Hall's Method

The grading margin result for the relay pairs of R3-R2 and R2-R1 (when graded using Hall's Method) from Appendix A are presented in probability density function in Figure 4.7 and cumulative distribution function in Figure 4.8 below.

Figure 4.7 indicates the percentage of the test cases with respect to the relay pair grading margin. The vertical y-axis of the graph represents the percentage out of the 162 test cases that are conducted in short circuit simulation under various power system dynamic scenarios discussed in Section 3.6. The horizontal x-axis of the graph represents the ranges of calculated grading margin for the relay pairs of R3-R2 and R2-R1 in all the 162 test cases which are tabulated in Appendix A. Each of the bars in the probability density function represents the percentage of test cases in which the grading margin of the relay pairs of R3-R2 and R2-R1 is between a particular range. Referring to Figure 4.7, there is 17.28% out of the 162 test cases in which the grading margin of the relay pairs of R3-R2 and R2-R1 is between 0s and 0.299s. For grading margin of the relay pairs of R3-R2 and R2-R1 between 0.3s and 0.599s, there is 24.07% out of the 162 test cases.

In Figure 4.8, the vertical y-axis of the graph represents the cumulative percentage of test cases. The horizontal x-axis of the graph represents all the grading margin for the relay pairs of R3-R2 and R2-R1. The observation from the graph is summarized into Table 4.12 which shows the number of occurrences for GM less than 0.3 and GM of 0.3 and above – using Hall's Method.

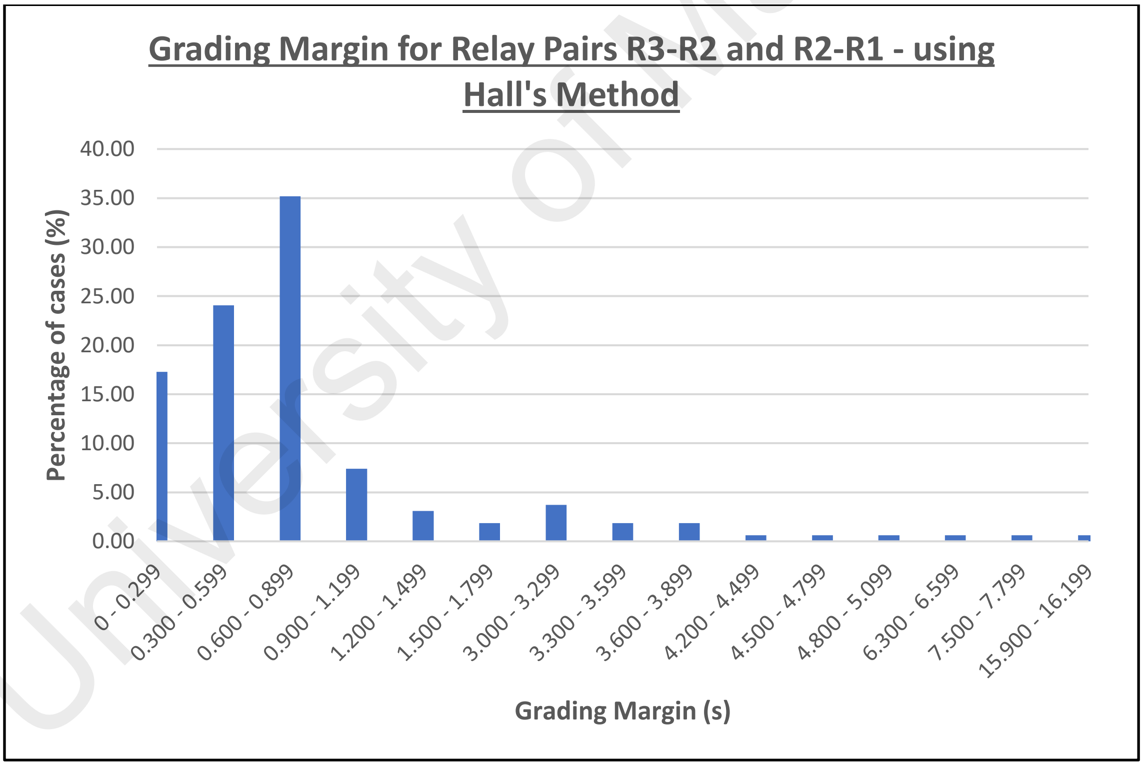

Figure 4. 7: Probability density function of grading margin for relay pairs R3-R2 and R2-R1 using Hall's Method.

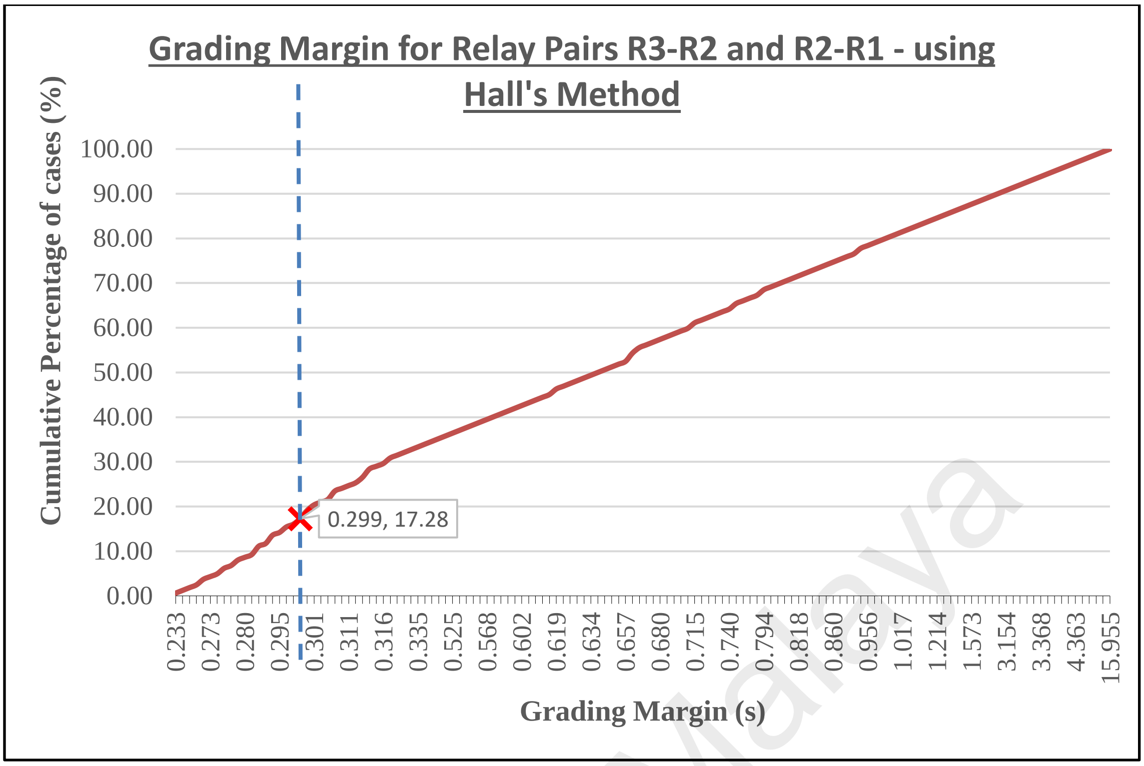

Figure 4. 8: Cumulative distribution function of grading margin for relay pairs R3-R2 and R2-R1 using Hall's Method.

The left column of Table 4.12 shows the grouping of the grading margin of the relay pairs. One group represents a grading margin less than 0.3s, and the other group represents a grading margin of 0.3s and above. The second column of Table 4.12 shows the number of occurrences and the last column reflects on the percentage of occurrence. From Table 4.12 below, it is deduced that there are 28 occurrences (17.28%) in which grading margin of the relay pairs is below 0.3s. As such, when a fault occurs, instead of the relay closest to the fault location operating and clearing the fault, there is 17.28% possibility that both main relay and backup relay will operate. As a result, more customers will experience disruptions in electricity supply due to the operation of backup relay. There are 134 occurrences (82.72%) in which the grading margin of the relay pairs is either equivalent or above 0.3s.

Table 4.12: Number of occurrences for GM less than 0.3 and GM of 0.3 and above – using Hall's Method.

Grading margin (s)	Number of cases	Percentage (%)
Less than 0.3s	28	17.28
0.3s and above	134	82.72

4.5.4.2 Ravindranath's Method

The grading margin result for the relay pairs of R3-R2 and R2-R1 (when graded using Ravindranath's Method) from Appendix A are presented in probability density function in Figure 4.9 and cumulative distribution function in Figure 4.10 below.

Figure 4.9 indicates the percentage of the test cases with respect to the relay pair grading margin. The vertical y-axis of the graph represents the percentage out of the 162 test cases that are conducted in short circuit simulation under various power system dynamic scenarios discussed in Section 3.6. The horizontal x-axis of the graph represents the ranges of calculated grading margin for the relay pairs of R3-R2 and R2-R1 in all the 162 test cases which are tabulated in Appendix A. Each of the bars in the probability density function represents the percentage of test cases in which the grading margin of the relay pairs of R3-R2 and R2-R1 is between a particular range. Referring to Figure 4.9, there is 0% out of the 162 test cases in which the grading margin of the relay pairs of R3-R2 and R2-R1 is between 0s and 0.299s. For grading margin of the relay pairs of R3-R2 and R2-R1 between 0.3s and 0.599s, there is 39.51% out of the 162 test cases.

In Figure 4.10, the vertical y-axis of the graph represents the cumulative percentage of test cases. The horizontal x-axis of the graph represents all the grading margin for the relay pairs of R3-R2 and R2-R1. The observation from the graph is summarized into

Table 4.13 which shows the number of occurrences for GM less than 0.3 and GM of 0.3 and above – using Hall's Method.

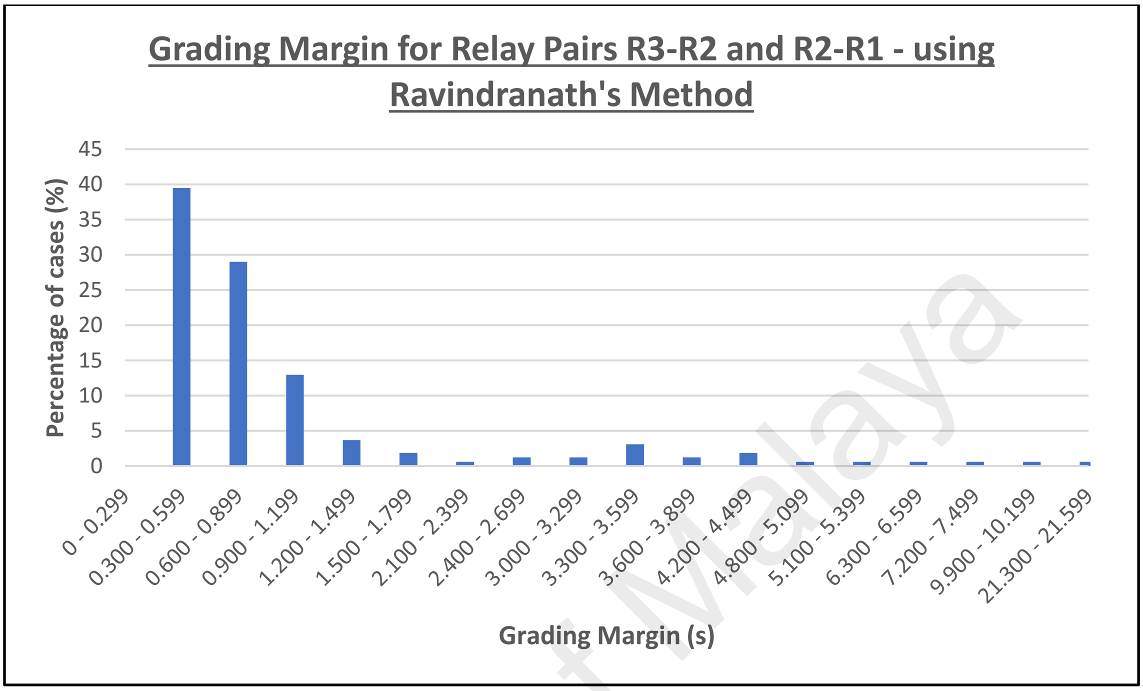

Figure 4. 9: Probability density function of grading margin for relay pairs R3-R2 and R2-R1 using Ravindranath's Method.

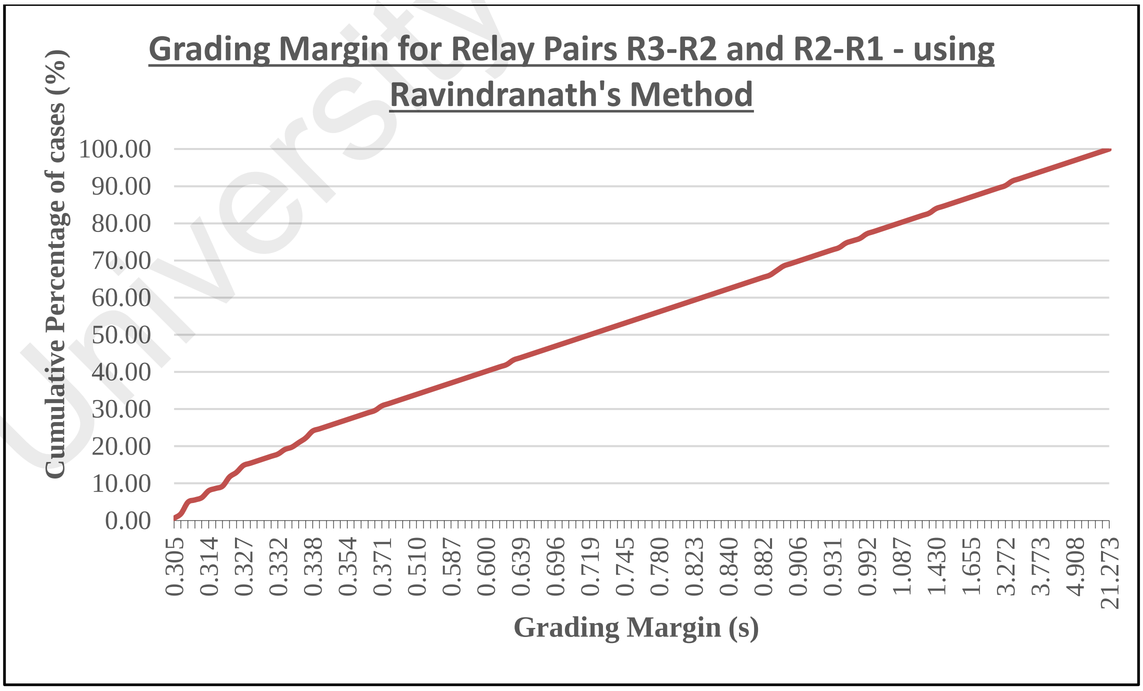

Figure 4. 10: Cumulative distribution function of grading margin for relay pairs R3-R2 and R2-R1 using Ravindranath's Method.

The left column of Table 4.13 shows the grouping of the grading margin of the relay pairs. One group represents a grading margin less than 0.3s and the other group represents a grading margin of 0.3s and above. The second column of Table 4.13 shows the number of occurrences and the last column reflects on the percentage of occurrence. From Table 4.13 below, it is deduced that there are zero occurrences (0%) in which grading margin of the relay pairs is below 0.3s. In all 162 cases, the grading margin of the relay pairs is either equivalent or above 0.3s. This implies that the relay pair grading margin is never jeopardized. As such, when a fault occurs, only the relay closest to the fault location will operate and clear the fault.

Table 4.13: Number of occurrences for GM less than 0.3 and GM of 0.3 and above – using Ravindranath's Method.

Grading margin (s)	**Number of cases**	**Percentage (%)**
Less than 0.3	0	0
0.3 and above	162	100

The number of occurrences for GM less than 0.3 and GM of 0.3 and above from the 162 cases as a result when using Hall's Method and Ravindranath's Method to grade the overcurrent main-backup relay pairs is summarized in Table 4.14. From Table 4.14, it is clearly shown that when using Hall's Method to grade the relays, there are 28 cases (17.28%) in which the grading margin is below 0.3s indicating that relay grading margin is jeopardized. In contrast, when using Ravindranath's Method to grade the relays, all calculated grading margin are 0.3 seconds and above for all the 162 cases (100%), which proved that the integrity of grading margin is secured.

Table 4.14: Number of occurrences for GM less than 0.3 and GM of 0.3 and above – using Hall's Method and Ravindranath's Method.

	Hall's Method		**Ravindranath's Method**	
Grading margin (s)	**Number of cases**	**Percentage (%)**	**Number of cases**	**Percentage (%)**
Less than 0.3	28	17.28	0	0
0.3 and above	134	82.72	162	100

4.6 Validation of the simulation results through real-time Hardware-in-the-Loop (HIL) experiment using OPAL-RT simulator

The theoretical findings from the simulation using Simulink are validated through real-time HIL experiment using the OPAL-RT simulator. Out of the 162 test cases, Test no. 73 has been selected for the experimental explanation in this section.

4.6.1 Hall's Method

Figure 4.11 shows the signals from relay R1 and relay R2 viewed from the OPAL-RT ScopeView. As discussed in Section 3.8.2, the digital output of the relays are connected to the digital input of the real-time simulator. Hence, the signals from relay R1 and relay R2 as well as the fault signal viewed in ScopeView are digital signals. The digital signals recorded are based on 1 (on) or 0 (off). The first monitoring channel (at the top) shows the fault signal. The second monitoring channel shows the signal from the main relay R2. The last monitoring channel (at the bottom) shows the signal from the backup relay R1.

From the ScopeView, the fault is seen to be initiated at time t = 4.8671s. At time t = 4.8671s, the fault signal changes from 0 (off) to 1 (on). In Simulink simulator environment, the fault is introduced at time t = 5s. This is due to a computation delay in Simulink simulator environment. Therefore, in OPAL-RT simulator environment, the time shown in the scope is slightly different as compared to the time in Simulink simulator environment.

From the second monitoring channel, when the fault is introduced at time t = 4.8671s, the signal from main relay R2 changes from 1 (on) to 0 (off) at time t = 4.9171s. The change in signal from 1 (on) to 0 (off) indicates the main relay R2 has operated. The digital input of the real-time simulator will detect the trip signal from R2 and opens the circuit breaker at PPU 2 in the simulator environment.

From the last monitoring channel, the signal from backup relay R1 also changes from 1 (on) to 0 (off) at time t = 5.0967s. The change in signal from 1 (on) to 0 (off) indicates the main relay R1 has operated. The digital input of the real-time simulator will detect the trip signal from R1 and opens the circuit breaker at PPU 1 in the simulator environment.

Observation on the relay signals from both the second and last monitoring channels has shown both main relay R2 and backup relay R1 have operated. This shows that the grading margin has been jeopardized.

Through the HIL experiment, the generated results as observed in the RT-LAB simulator environment are similar to the Simulink simulation result tabled in Appendix A for all the main and backup relay pairs, R3-R2 and R2-R1 graded using Hall's Method.

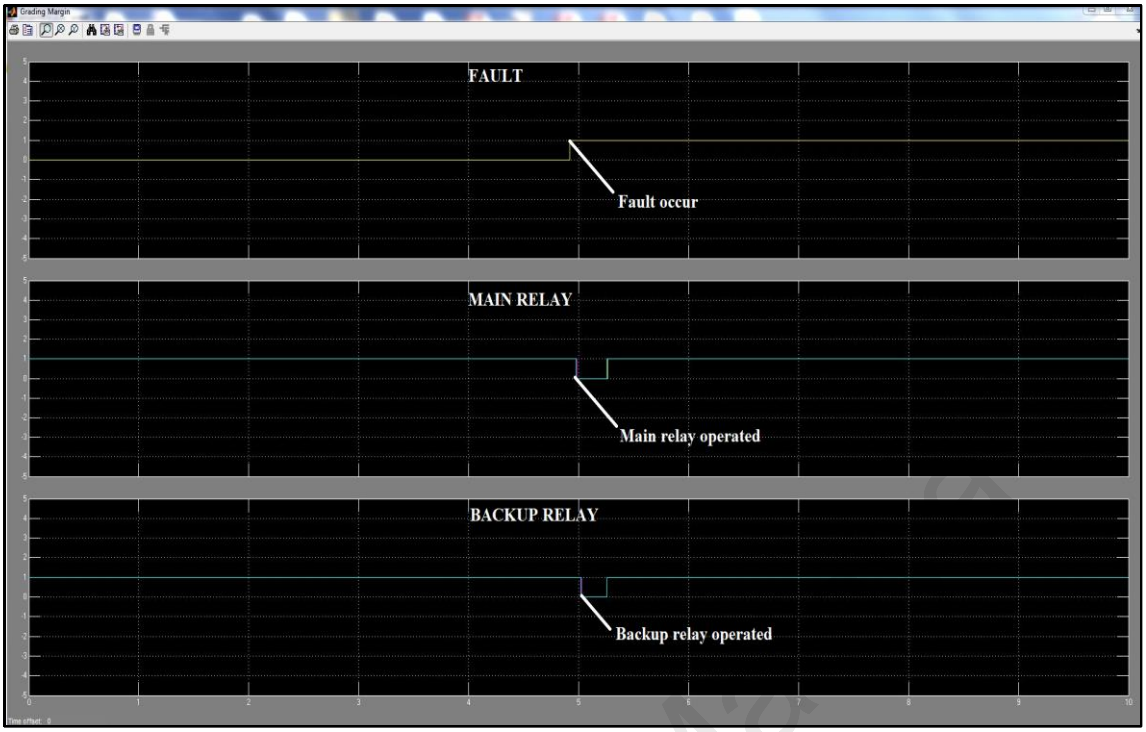

Figure 4. 11: Signals from relay R1 and relay R2 from OPAL-RT ScopeView – using Hall's Method.

4.6.2 Ravindranath's Method

Figure 4.12 shows the signals from relay R1 and relay R2 viewed from the OPAL-RT ScopeView. As discussed in Section 3.8.2, the digital output of the relays are connected to the digital input of the real-time simulator. Hence, the signals from relay R1 and relay R2 as well as the fault signal viewed in ScopeView are digital signals. The digital signals recorded are based on 1 (on) or 0 (off). The first monitoring channel (at the top) shows the fault signal. The second monitoring channel shows the signal from the main relay R2. The last monitoring channel (at the bottom) shows the signal from the backup relay R1.

From the ScopeView, the fault is seen to be initiated at time t = 4.8671s. At time t = 4.8671s, the fault signal changes from 0 (off) to 1 (on).

From the second monitoring channel, when the fault is introduced at time t = 4.8671s, the signal from main relay R2 changes from 1 (on) to 0 (off) at time t = 5.2006s. The change in signal from 1 (on) to 0 (off) indicates the main relay R2 has operated. The digital input of the real-time simulator will detect the trip signal from R2 and opens the circuit breaker at PPU 2 in the simulator environment.

From the last monitoring channel, the signal from backup relay R1 maintains at 1 (on). This observation indicates the backup relay R1 did not operate. The digital input of the real-time simulator did not detect any trip signal from R1. Therefore, the circuit breaker at PPU 1 remains in closed position in the simulator environment.

From the monitoring scope extracted from the RT-LAB simulator environment, only main relay R2 has operated. This shows that the grading margin is not jeopardized.

Through the HIL experiment, the generated results as observed in the RT-LAB simulator environment are similar to the Simulink simulation result tabled in Appendix A for all the main and backup relay pairs, R3-R2 and R2-R1 graded using Ravindranath's Method.

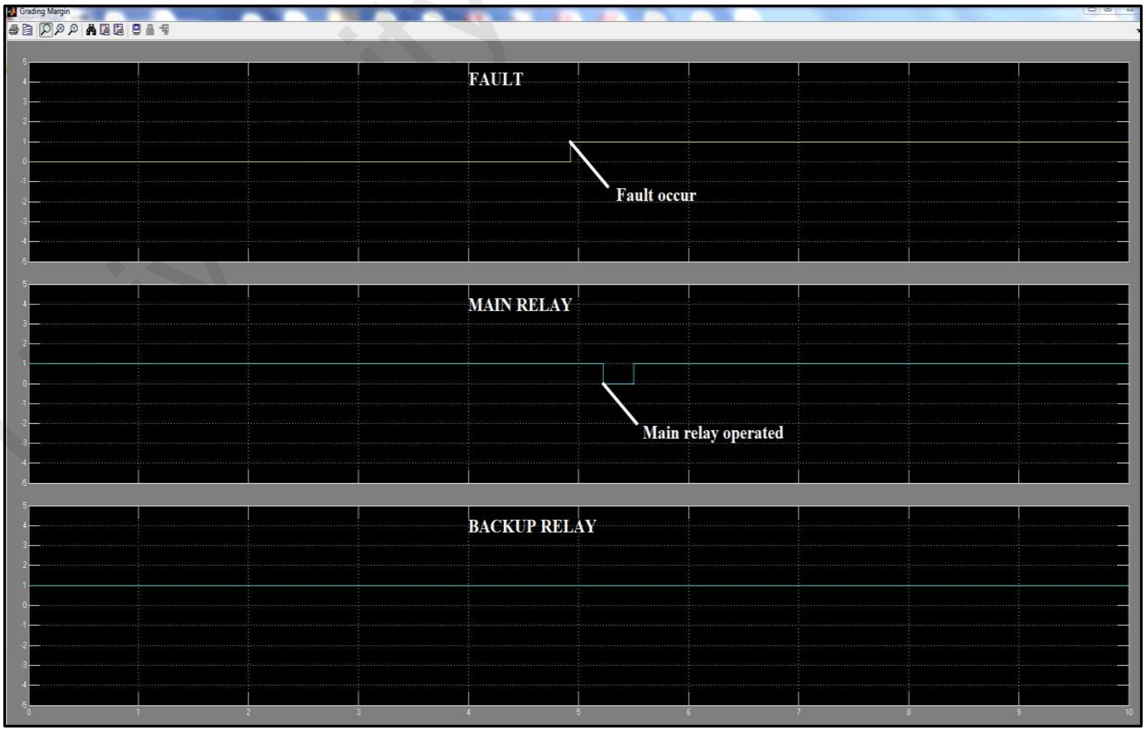

Figure 4. 12: Signals from relay R1 and relay R2 from OPAL-RT ScopeView – using Ravindranath's Method.

4.7 Summary of Chapter

In this chapter, the results for the research study have been presented and the findings are discussed. First, the results of the short circuit analysis in conventional radial 33kV distribution network is presented. Next, the overcurrent relay grading in the conventional distribution network is performed using Hall's Method and Ravindranath's Method. The overcurrent relay settings for both the relay grading methods are presented. This is followed by the presentation of the results for grading margin between all main-backup relay pairs with model being simulated under various power system scenario. It was found that when using Hall's Method to grade the relays, there are 28 cases (17.28%) in which the grading margin is below 0.3s indicating that relay grading margin is jeopardized. In contrast, when using Ravindranath's Method to grade the relays, all calculated grading margin are 0.3 seconds and above for all the 162 cases (100%), which proved that the integrity of grading margin is secured. The theoretical findings from the simulation using Simulink are then validated through real-time HIL experiment using the OPAL-RT simulator. Through the HIL experiment, the generated results are similar to the results obtained from the Simulink simulation for all the main and backup relay pairs, R3-R2 and R2-R1 which are tabled in Appendix A.

CHAPTER 5: CONCLUSION

5.1 Conclusion

This project aims to apply two different methods of overcurrent relay grading that is practiced in the industry. One of the relay grading methods is proposed by (Hall Stephens, 1998) and the other relay grading method is proposed by (Ravindranath & Chander, 1977).

The project has considered a 33kV radial distribution network. First, the two different methods of overcurrent relay grading have been applied to grade the overcurrent relays R1, R2, and R3 in this research work. Time multiplier setting (TMS) for the respective R1, R2, and R3 for both Hall's Method and Ravindranath's Method have been successfully calculated and tabulated. These TMS values are used for the relay settings. As such, Objective 1 to apply the two different methods of overcurrent relay grading practiced in the industry has been achieved.

Subsequently, using the TMS values to set the relays R1, R2, and R3, simulations were conducted under various power systems dynamic scenarios such as a change in load size, cable length, fault resistance, and fault location. Using the short circuit current recorded through these simulations, the grading margin for main-backup relay pairs of R3-R2 and R2-R1 have been calculated and compared for both relay grading methods. When Hall's Method is used to grade the overcurrent main-backup relay pairs, out of a total of 162 test cases, there are 28 cases (17.28%) in which the grading margin is below 0.3 seconds which proved that the grading margin has been jeopardized. In contrast, when using Ravindranath's Method to grade the overcurrent relays, all the calculated grading margin are 0.3 seconds and above, which proved that the integrity of grading margin is secured. As such, Objective 2 to investigate the main-backup relays grading margin for the two methods of overcurrent relay grading under the various power system dynamic scenarios has been achieved.

Lastly, all the simulation results are validated through real-time hardware experiment using OPAL-RT simulator. The ScopeView tool in RT-LAB software has been utilized to compare the result of relay signals for the main relay and backup relay when a fault occurs in both the cases of using Hall's Method and Ravindranath's Method. The HIL experiment generated similar results in the RT-LAB simulator environment in comparison to the results obtained from the Simulink simulation which are tabled in Appendix A. As such, Objective 3 to validate the theoretical findings through real-time Hardware-in-the-Loop (HIL) experiment using OPAL-RT simulator has also been achieved.

In summary, all objectives listed in Chapter 1 have been achieved, and the problem statement has been achieved in this project.

5.2 Contributions of research

Discovery that the grading margin may be jeopardized if relays are graded with Hall's Method

There have been two different methods of grading overcurrent relays being practiced in the industry. One of the grading methods is proposed by (Hall Stephens, 1998) whereas the other relay grading method is proposed by (Ravindranath & Chander, 1977). Through this investigation, main-backup relay pairs should be graded using Ravindranath's Method, instead of Hall's Method. If relay pairs are graded incorrectly, the grading margin between the relay pairs will be jeopardized. While there are cases in this investigation in which the grading margin between the relay pairs is 0.3s and above when the Hall's Method is being adopted, the probability of 17.28% for jeopardized grading margin should not be neglected. If Ravindranath's Method is used, then there will be no grading margin jeopardized.

5.3 Recommendations for Future Work

This project has concluded that when overcurrent relays are graded using Hall's Method, grading margin of the relay pairs will have the possibility of being jeopardized, which is as high as 17.28%. When using Ravindranath's Method to grade the overcurrent relays, the grading margin of the relay pairs is 0%. However, the above conclusion only considered the same current transformer (CT) ratio for relay R1, relay R2 and relay R3. For future research work, varied CT ratio can be considered for the relay R1, relay R2, and relay R3. With varied CT ratio for each relay, the grading margin for the relay pairs of R3-R2 and R2-R1 should then be re-calculated.

In this research work, the characteristic of the Mikro MK3000L relay is Standard Inverse (SI). Future research can be conducted to evaluate the impact of using different standard characteristics of the Mikro MK3000L relay such as the Very Inverse (VI) and Extremely Inverse (EI) on the grading margin of the relay pairs.

REFERENCES

ALSTOM. (2011). *Network Protection & Automation Guide*: ALSTOM.

Anderson, P. M. (1995). *Analysis of faulted power systems*: IEEE Press.

Anderson, P. M. (1999). *Power System Protection*: McGraw-Hill.

Association, E. T., & Engineers, I. o. E. (1995). *Power System Protection: Systems and Methods*: Institution of Engineering and Technology.

Blackburn, J. L., & Domin, T. J. (2014). *Protection Relaying: Principles and Applications, Fourth Edition*: Taylor & Francis.

Das, J. C. (2017). *Power System Protection Relaying*: CRC Press.

Distribution, T. N. B. (2011). *Electricity Supply Application Handbook* (Third Edition ed.): TNB Distribution Division.

Ekanayake, J. B. (2008). A Systematic Approach for Phase-Fault Over-Current Protection Coordination of Complex Networks. *International Journal of Electrical Engineering Education, 45*(3), 229-238. doi:10.7227/ijeee.45.3.4

Elmore, W. A. (2003). *Protection Relaying: Theory and Applications*: CRC Press.

Glover, J. D., & Sarma, M. S. (1994). *Power System Analysis and Design: With Personal Computer Applications*: International Thomson Publishing Company.

Grainger, J. J., & Stevenson, W. D. (1994). *Power system analysis*: McGraw-Hill.

Hall Stephens, J. (1998). *Kempe's Engineers Yearbook*: CMP Information Limited.

Hindle, P. J., & Sanderson, J. V. H. (1997, 25-27 March 1997). *Overcurrent protection co-ordination: a modern approach for modern devices.* Paper presented at the Sixth International Conference on Developments in Power System Protection (Conf. Publ. No. 434).

Hodgkiss, J. W. (1995). Overcurrent protection. In Power System Protection 2: Systems and methods Energy Engineering (pp. 1-65): Institution of Engineering and Technology. Retrieved from http://digital-library.theiet.org/content/books/10.1049/pbpo905g_ch8. doi:doi:10.1049/PBPO905G_ch8

Horowitz, S. H., & Phadke, A. G. (2014). *Power System Relaying, Fourth Edition*: John Wiley & Sons Limited.

Hussin, N. H., Idris, M. H., Amirruddin, M., Ahmad, M. S., Ismail, M. A., Abdullah, F. S., & Mukhta, N. M. (2016). *Modeling and simulation of inverse time overcurrent relay using Matlab/Simulink.* Paper presented at the 2016 IEEE International Conference on Automatic Control and Intelligent Systems (I2CACIS).

IEEE. (1994). IEEE Recommended Practice for Electric Power Distribution for Industrial Plants. *IEEE Std 141-1993*, 1-768. doi:10.1109/IEEESTD.1994.121642

IEEE. (1997). IEEE Standard Inverse-Time Characteristic Equations for Overcurrent Relays. *IEEE Std C37.112-1996*, i. doi:10.1109/IEEESTD.1997.81576

IEEE. (1998). IEEE Recommended Practice for Industrial and Commercial Power Systems Analysis (Brown Book). *IEEE Std 399-1997*, 1-488. doi:10.1109/IEEESTD.1998.88568

IEEE. (2001). IEEE Recommended Practice for Protection and Coordination of Industrial and Commercial Power Systems (IEEE Buff Book). *IEEE Std 242-2001 (Revision of IEEE Std 242-1986) [IEEE Buff Book]*, 1-710. doi:10.1109/IEEESTD.2001.93369

Kersting, W. H. (2001). *Radial distribution test feeders.* Paper presented at the 2001 IEEE Power Engineering Society Winter Meeting.

Kezunovic, M., Ren, J., & Lotfifard, S. (2016). Basics of Protective Relaying and Design Principles. In *Design, Modeling and Evaluation of Protective Relays for Power Systems* (pp. 45-76): Springer.

Kezunovic, M., Ren, J., & Lotfifard, S. (2016). Testing of Digital Protective Relays. In *Design, Modeling and Evaluation of Protective Relays for Power Systems* (pp. 263-297): Springer.

Lakervi, E., & Holmes, E. J. (1995). *Electricity Distribution Network Design*: P. Peregrinus.

Mason, C. R. (1956). *The Art & Science of Protection Relaying*: Wiley.

Mercede, F. (2009). Fault Calculations in Industrial/Commercial Power Systems - IEEE Red Book Self-Study Course. *IEEE/EAB 193 Self-Study Course - IEEE Red Book*, c1-636. doi:10.1109/IEEESTD.2009.4838997.

Mehta, P., & Makwana, V. (2017). *Modelling of overcurrent relay with inverse characteristics for radial feeder protection using graphical user interface.* Paper presented at the 2017 International Conference on Intelligent Computing, Instrumentation and Control Technologies (ICICICT).

Paithankar, Y. G., & Bhide, S. R. (2011). *Fundamentals of Power System Protection*: PHI Learning.

Prakash, K., Lallu, A., Islam, F. R., & Mamun, K. A. (2016). *Review of Power System Distribution Network Architecture.* Paper presented at the 2016 3rd Asia-Pacific World Congress on Computer Science and Engineering (APWC on CSE).

Prévé, C. (2013). Different Selectivity Systems. In *Protection of Electrical Networks*: Wiley.

Ravindranath, B., & Chander, M. (1977). *Power System Protection and Switchgear*: Wiley Eastern Limited.

Saadat, H. (2011). *Power System Analysis*: PSA Publishing LLC.

Sallam, A. A., & Malik, O. P. (2011). Protection of Electric Distribution Systems. In *Electric Distribution Systems* (pp. 163-235): Wiley.

van C. Warrington, A. R. (1977). *Protection Relays Their Theory and Practice: Volume Two*: Springer.

Vandiver, B. (2016, 4-7 April 2016). *Why testing digital relays are becoming so difficult! Part 3 advanced feeder protection.* Paper presented at the 2016 69th Annual Conference for Protective Relay Engineers (CPRE).

Webster, J. G., & Das, R. (2017). Overcurrent Protection. In *Wiley Encyclopedia of Electrical and Electronics Engineering*: Wiley.